Neurobiology of Aging 137 (2024) 62–77

Contents lists available at ScienceDirect

Neurobiology of Aging

journal homepage: www.elsevier.com/locate/neuaging.org

The association between posterior resting-state EEG alpha rhythms and functional MRI connectivity in older adults with subjective memory complaint

Susanna Lopez [a], Harald Hampel [b,1], Patrizia Andrea Chiesa [b,c,d], Claudio Del Percio [a], Giuseppe Noce [e], Roberta Lizio [a], Stefan J. Teipel [f,g], Martin Dyrba [f], Gabriel González-Escamilla [h], Hovagim Bakardjian [c,i,j], Enrica Cavedo [b], Simone Lista [b], Andrea Vergallo [b], Pablo Lemercier [b,i,j], Giuseppe Spinelli [i,j], Michel J. Grothe [g], Marie-Claude Potier [d], Fabrizio Stocchi [k,l], Raffaele Ferri [m], Marie-Odile Habert [i,j,n], Bruno Dubois [c,d], Claudio Babiloni [a,o,*,1], INSIGHT-preAD study group

[a] Department of Physiology and Pharmacology "Erspamer", Sapienza University of Rome, Rome, Italy
[b] Sorbonne University, GRC n° 21, Alzheimer Precision Medicine (APM), AP-HP, Pitié-Salpêtrière Hospital, Boulevard de l'hôpital, Paris F-75013, France
[c] Institute of Memory and Alzheimer's Disease (IM2A), Department of Neurology, Pitié-Salpêtrière Hospital, AP-HP, Boulevard de l'hôpital, Paris F-75013, France
[d] Institut du Cerveau et de la Moelle épinière, ICM, INSERM U1127, CNRS UMR 7225, Sorbonne Université, Paris F- 75013, France
[e] IRCCS Synlab SDN, Naples, Italy
[f] Department of Psychosomatic Medicine, University of Rostock, Rostock, Germany
[g] German Center for Neurodegenerative Diseases (DZNE), Greifswald, Rostock, Germany
[h] Department of Neurology, Focus Program Translational Neuroscience (FTN), Rhine-Main Neuroscience Network (rmn2), University Medical Center of the Johannes Gutenberg University Mainz, Mainz, Germany
[i] Centre pour l'Acquisition et le Traitement des Images, (CATI platform), France
[j] Laboratoire d'Imagerie Biomédicale, CNRS, INSERM, Sorbonne University, LIB, Paris F-75006, France
[k] IRCCS San Raffaele, Rome, Italy
[l] Telematic University, San Raffaele, Rome, Italy
[m] Oasi Research Institute - IRCCS, Troina, Italy
[n] AP-HP, Pitié-Salpêtrière Hospital, Department of Nuclear Medicine, Paris F-75013, France
[o] San Raffaele Cassino, Cassino, FR, Italy

ARTICLE INFO

Keywords:
Resting state EEG rhythms
Alpha rhythms
Preclinical Alzheimer's disease (AD)
Preclinical Alzheimer's neuropathology
Subjective Memory Complaint (SMC)
Functional Magnetic Resonance Imaging (fMRI) connectivity
Cognitive Reserve
INSIGHT-Pre-AD study

ABSTRACT

Resting-state eyes-closed electroencephalographic (rsEEG) alpha rhythms are dominant in posterior cortical areas in healthy adults and are abnormal in subjective memory complaint (SMC) persons with Alzheimer's disease amyloidosis. This exploratory study in 161 SMC participants tested the relationships between those rhythms and seed-based resting-state functional magnetic resonance imaging (rs-fMRI) connectivity between thalamus and visual cortical networks as a function of brain amyloid burden, revealed by positron emission tomography and cognitive reserve, measured by educational attainment. The SMC participants were divided into 4 groups according to 2 factors: Education (Edu+ and Edu-) and Amyloid burden (Amy+ and Amy-). There was a statistical interaction ($p < 0.05$) between the two factors, and the subgroup analysis using estimated marginal means showed a positive association between the mentioned rs-fMRI connectivity and the posterior rsEEG alpha rhythms in the SMC participants with low brain amyloidosis and high CR (Amy-/Edu+). These results suggest that in SMC persons, early Alzheimer's disease amyloidosis may contrast the beneficial effects of cognitive reserve on neurophysiological oscillatory mechanisms at alpha frequencies and connectivity between the thalamus and visual cortical networks.

* Correspondence to: Department of Physiology and Pharmacology "V. Erspamer" Sapienza University of Rome, P. le A. Moro 5, Rome 00185, Italy.
E-mail address: claudio.babiloni@uniroma1.it (C. Babiloni).
[1] Equally contributing authors.

https://doi.org/10.1016/j.neurobiolaging.2024.02.008
Received 25 May 2020; Received in revised form 9 February 2024; Accepted 19 February 2024
Available online 28 February 2024

1. Introduction

It is well-known that in patients with Alzheimer's disease (AD) and high education attainment, cognitive performance is typically better than expected based on the burden of brain neuropathology and neurodegeneration (Stern et al., 2018). This resilience of the cognitive status was attributed to a sort of cognitive reserve (CR) accumulated by persons with high education attainment whose life is typically characterized by many occasions and opportunities to learn new knowledge and exercise cognitive functions in their job and social environment (Arenaza-Urquijo et al. 2015 and Stern et al. 2018).

The neural basis of CR would rely on protective and compensatory mechanisms inducing effective recruitment and interactions among brain neural populations (Arenaza-Urquijo et al. 2015, Stern et al. 2018). These mechanisms are considered ***protective*** in healthy older adults based on previous evidence showing that high education attainment is typically associated with a delayed onset of dementia onset over aging in those adults (Bennett et al., 2014; Valenzuela and Sachdev, 2006; Sachdev, Valenzuela, 2009; Reed et al., 2010; Buchman and Bennett, 2012; Zahodne et al., 2013, 2015; Stern, 2012; Arenaza-Urquijo and Vemuri, 2018; Garibotto et al., 2008; Morbelli and Nobili, 2014; Stern et al., 2018; Hampel et al., 2019). At the same time, they are considered ***compensatory*** in AD patients based on previous evidence showing that even if the global cognitive status is equal, AD patients with high education attainment are typically characterized by greater brain atrophy as whether their cognitive neural systems were more resilient to the neuropathological and neurodegenerative burden (Stern et al., 2018).

The neural mechanisms underlying the CR can be conceptualized as a sort of **brain reserve**. Concretely, the brain reserve may include greater brain size, white matter integrity, cerebrovascular health, synapsis density, and dendritic branching (Foubert-Samier et al., 2012; Cammisuli et al., 2022). Globally, they will allow good neural efficiency and capacity even when a certain degree of neuropathology and neurodegeneration can be observed (Pettigrew and Soldan, 2019). Enhanced brain functional connectivity patterns would also characterize the brain reserve. Resting-state functional magnetic resonance imaging (rs-fMRI) studies showed that CR proxies (e.g., educational attainment) were positively related to an enhanced cortical default mode network (DMN) and cognitive performances in healthy seniors (Arenaza-Urquijo et al., 2013). They were also positively correlated with enhanced functional connectivity in the posterior cingulate cortex (PCC) and temporal lobes in patients with dementia due to AD (Bozzali et al., 2015). Furthermore, they were positively correlated with enhanced functional connectivity in prefrontal, premotor areas, and parietal networks in healthy controls (Franzmeier et al., 2018a) and in patients with mild cognitive impairment (ADMCI) and dementia (Serra et al., 2015; Franzmeier et al., 2017a, b; Franzmeier et al., 2018b).

The brain reserve includes neurophysiological brain oscillatory mechanisms regulating the vigilance and wake-sleep transitions probed by the recording of ***resting-state electroencephalographic*** (rsEEG) rhythms. In previous studies, the CR (e.g., years of education and verbal IQ scores) was positively related to the spectral coherence of posteriorly dominant rsEEG alpha rhythms (8–12 Hz) between electrodes placed at occipital and other scalp regions in young and old healthy persons, reflecting interrelated synchronization of neural activity between cortical areas (Fleck et al., 2017, 2019). The CR (i.e., educational attainment) was also positively related to posterior rsEEG alpha power density in the old cognitively unimpaired persons of the multicenter PDWAVES cohort (www.pdwaves.eu) (Babiloni et al., 2020a). Similar results were observed in persons with subjective memory complaints (SMC) and negative brain amyloid-β biomarkers of positron emission tomography (SMCneg) from the French INSIGHT cohort (Dubois et al., 2018). The CR (i.e., educational attainment) was positively related to posterior rsEEG alpha power density (Babiloni et al., 2020b). Those results could reflect neuroprotective mechanisms associated with the CR. Along the same line, the CR (i.e., educational attainment) was negatively related to the posterior rsEEG alpha power density in the ADMCI patients of the multicenter PDWAVES cohort (www.pdwaves.eu) (Babiloni et al., 2020a). Furthermore, the CR (i.e., educational attainment) was negatively related to posterior rsEEG alpha power density in the SMC persons with positive brain amyloid-biomarkers (SMCpos) of the French INSIGHT cohort (Babiloni et al., 2020b). Those results were speculatively explained in terms of compensatory mechanisms associated with the CR. Furthermore, they extended to the SMC condition previous findings in AD patients with MCI and dementia, pointing to the dependence of posterior rsEEG alpha rhythms from AD neuropathology. In those findings, amyloid β42, p-tau, and total tau levels from cerebrospinal fluid (CSF) were positively associated with widespread rsEEG alpha and beta rhythms in AD patients with MCI and dementia (Smailovic et al., 2018). Similarly, rsEEG alpha rhythms were associated with CSF p-tau and p-tau/Aβ42 in AD patients with MCI (Jovicich et al., 2019; Cecchetti et al., 2021) and dementia (Kouzuki et al., 2013).

The above data and considerations suggest that the brain reserve associated with the CR (e.g., education attainment) may be at least in part reflected by rsEEG alpha rhythms and the brain functional connectivity estimated from rs-fMRI. In humans, these two neurophysiological correlates were related to each other. Previous multimodal rsEEG-rs-fMRI studies showed a substantial association between posterior rsEEG alpha rhythms and rs-fMRI (BOLD) signals. In healthy adults, parietal-occipital rsEEG alpha rhythms were associated with rs-fMRI signal, positively in the thalamus and negatively in cortical visual regions (Feige et al., 2005; Goldman et al., 2002; Gonçalves et al., 2006; Moosmann et al., 2003; Jaeger et al. 2023). In cognitively intact older participants, the occipital rsEEG alpha reactivity during eye-opening was associated with lesions in the subcortical white-matter connectivity from the cholinergic basal forebrain to the occipital cortex as revealed by the MRI (Wan et al., 2019). Finally, this strict rsEEG-rs-fMRI relationship was also informative in the AD model. In ADMCI patients, abnormalities in the rsEEG theta/alpha rhythms were associated with reduced rs-fMRI connectivity from the posterior nodes of the cortical default mode network (Jovicich et al., 2019). In ADD patients, there was a loss of the normal positive association between the rsEEG alpha rhythms and the rs-fMRI signal in the posterior cortex (Brueggen et al., 2017). Notably, no previous studies tested the hypothesis of an association between posterior rsEEG alpha rhythms and fMRI signals in SMC persons at the preclinical stage of AD.

In the present study, we used the database of the INSIGHT cohort (Dubois et al., 2018) to test the novel hypothesis that in SMC persons, posterior rsEEG alpha rhythms may be associated with the functional connectivity in the visual thalamus-cortical network as a part of the brain reserve due to the CR (i.e., educational attainment). Such association may be dependent on the brain amyloid burden and structural integrity. To test that hypothesis, an advanced multimodal methodological approach included biomarkers derived from rsEEG recordings, amyloid positron emission tomography (amyPET), structural MRI, and rs-fMRI.

2. Materials and Methods

The general methodology of the EEG data analysis used in the present study has been developed in the framework of a research line of the Eurasian PDWAVES Consortium (www.pdwaves.eu). This research line aims to contribute to a better understanding of the neurophysiological brain oscillatory mechanisms underlying the regulation of vigilance as a relevant layer of information on the traditional neurobiological and neuroanatomical AD model. That EEG methodology allowed the comparability of the results of the research line across the experimental series. More explanations of the methodology and previous representative results can be found elsewhere (Babiloni et al., 2017, 2018a, 2018b, 2020, 2021, 2022a, 2022b).

2.1. Participants

Participants were recruited at the Pitié-Salpêtrière University Hospital in Paris, France, in the framework of the INSIGHT-preAD study to investigate the earliest preclinical stages of AD and its development, including influencing factors and markers of disease progression (Dubois et al., 2018). The INSIGHT-preAD study currently includes baseline data in 318 cognitively intact individuals, between 70 and 85 years old, with SMC status confirmed by an affirmative answer to both of the following questions: 1) "Are you complaining about your memory?" and 2) "Is it a regular complaint which lasts more than six months"? Indeed, cognition was unimpaired as revealed by MMSE score $\geq$ 27, Clinical Dementia Rating score equal to 0, and no evidence of episodic memory deficit measured by the total recall at the Free and Cued Selective Reminding Test (mean 46.1 $\pm$ 2.0; Dubois et al., 2018).

At the baseline recording session, other measurements (i.e., demographic, cognitive, functional, nutritional, biological, genetic, genomic, imaging, electrophysiological, etc.) were performed (see Dubois et al., 2018 for details).

All experiments were performed with each participant or caregiver's informed and overt consent, per the Code of Ethics of the World Medical Association (Declaration of Helsinki) and the standards established by the local Institutional Review Board. Local institutional Ethics Committee approved data sharing for scientific purposes.

2.2. Amyloid Positron emission tomography (amyPET) data acquisition and processing for participants' grouping

The SMC participants were stratified into two groups labeled amyloid-positive (SMCpos) and amyloid-negative (SMCneg), using the standard diagnostic markers of Alzheimer's neuropathology based on cortical-to-cerebellum standardized uptake value ratio (SUVR) from amyPET imaging.

PET scans were acquired 50 min after injection of 370 MBq (10 mCi) ^{18}F-florbetapir. Reconstructed PET images were analyzed with a pipeline developed by the CATI (http://cati-neuroimaging.com). Structural MRI images were co-registered to ^{18}Florbetapir-PET images using SPM8 (https://www.fil.ion.ucl.ac.uk/spm/software/spm8/) with visual inspection to detect any co-registration errors. Inverse deformation fields and matrix transformation from MRI data processing were used to derive composite cortical ROIs (left and right precuneus, posterior and anterior cingulate, parietal, temporal, and orbitofrontal cortex; according to Clark et al., 2012) and a reference region (in the pons and whole cerebellum) were placed in the individual native PET space. RBV-sGTM method was used to correct for the partial volume effect (Thomas et al., 2011). Parametric PET images were created for everyone by dividing each voxel with the mean activity extracted from the reference region.

SUVR values were calculated by averaging the mean activity of all the cortical ROIs in the individual PET native space. The two groups (SMCneg, N = 230, SMCpos, N = 88) were defined using the specific SUVR threshold of 0.79 to determine abnormality uptake identified in previous investigations of this Workgroup focused on those biomarkers (Habert et al., 2018; Chiesa et al., 2019a, b). Those procedures identified a more conservative (0.88) and a more liberal (0.79) threshold. The more conservative threshold was used in the previous reference study investigating functional brain connectivity from rsEEG alpha and beta rhythms in the INSIGHT-preAD cohort (Teipel et al., 2018). The liberal threshold has been adopted for several parallel rsEEG and neuroimaging studies in the INSIGHT-preAD cohort (Dubois et al., 2018). Therefore, for the present study, we opted for the value of 0.79 for the main rsEEG data analysis.

2.3. Stratification of the subjective memory complaint (SMC) seniors based on the education attainment

As a proxy of the CR, we used the education attainment score adopted in the original INSIGHT-preAD project protocol (Dubois et al., 2018). In this score, the level of education ranged from 1 to 8; 1 means the attendance of the only infant school (8 years of education), and 8 means the attendance of a higher education level in the population (i.e., bachelor, master's degree, or doctorate; at least 16 years of education). Based on this score, all SMC participants were stratified according to the median value computed in two sub-groups. The SMC participants with a low-to-moderate education level, from 1 to 6 of the education attainment score, were denoted as SMC Edu-. In contrast, the SMC participants with education attainment scores ranging from 7 to 8 were marked as SMC Edu+ (Dubois et al., 2018).

2.4. Magnetic resonance imaging (MRI) acquisition and preprocessing

For the cortical signature of the SMC participants, MRI acquisitions of the brain were conducted using a 3 Tesla scanner with parallel imaging capabilities (Siemens Magnetom Verio, Siemens Medical Solutions, Erlangen, Germany). The scanner used a quadrature detection head coil with 12 channels (transmit-receive circularly polarized CP-head coil). For the anatomical study, 3D TurboFLASH sequences were performed (orientation sagittal; repetition time [TR] = 2300 ms; echo time [TE] = 2.98 ms; inversion time = 900 ms; flip angle = 9°; 176 slices; slice thickness = 1 mm; field of view = 256*240 mm; matrix = 256*240; bandwidth = 240 Hz/Px). Cavedo et al. (2018) reported the technical details concerning the preprocessing for the cortical signature of prodromal AD and the automated calculation of HP and BF volumes.

2.5. Resting-state functional MRI (rs-fMRI) acquisition and preprocessing for seed-to-seed connectivity estimate

The SMC participants were tested for the specific association between the posterior rsEEG alpha rhythms and the rs-fMRI-based functional connectivity from subcortical and visual cortical networks relevant to their generation.

Scanning was performed on a 3-T Verio system MRI with the 12-channel head coil (Siemens Medical Systems, Erlangen, Germany) at the Center for Neuroimaging Research (Centre de NeuroImagerie de Recherche, CENIR) at the Brain & Spine Institute (ICM, CNRS/Inserm/Sorbonne Université), Pitié-Salpêtrière University Hospital, Paris, France. During the rs-fMRI scan, participants were instructed to keep their eyes closed and stay as still as possible.

The rs-fMRI images were collected by using an echo-planar imaging sequence (TR=2460 ms, TE=30 ms, slice thickness=3 mm, matrix=64×64, voxel size=3×3×3 mm, number of volumes=250, number of slices=45, run=1). The rs-fMRI data were preprocessed using Data Processing Assistant for Resting-State fMRI (DPARSF, Yan et al., 2016) implemented in Data Processing & Analysis for Brain Imaging (DPABI, available at http://rfmri.org/dpabi), based on SPM8. The first ten volumes for each participant were excluded to avoid potential noise related to the equilibrium of the magnet and the participant's adaptation to the scanner. The remaining 240 volumes were preprocessed in steps, including slice-timing correction, realignment, and segmentation using SPM priors for cerebrospinal fluid (CSF) and white matter. We regressed out the global mean and the confounding effects of CSF and white matter to reduce the impact of physiological noise. The Friston 24-parameter model, which includes six head motion parameters, six head motion parameters one-time point before, and the 12 corresponding squared items, was used to regress out head motion effects (Friston et al., 1996). The maximum displacement allowed was >2.5 mm in one or more orthogonal directions or >2.5° rotation. The motion-corrected functional volumes were spatially normalized to the T1 unified segmentation template in Montreal Neurological Institute coordinates derived from

SPM8 software and resampled to 3×3×3 mm voxels. A temporal bandpass filtering (bandpass 0.01–0.1 Hz) was applied to reduce the effect of low-frequency drift and high-frequency physiological noise. A smoothing procedure with a 4 mm FWHM Gaussian kernel was used.

Rs-fMRI functional connectivity was analyzed in a-priori selected regions of interest (ROIs) defined by the Automated Anatomical Labeling (AAL) atlas (Tzourio-Mazoyer et al., 2002). To test the specific association between posterior rsEEG alpha rhythms in the SMC participants and the connectivity from the cholinergic basal forebrain, thalamus, and core resting-state cortical networks relevant for the generation of posterior rsEEG alpha rhythms as a function of the brain amyloid burden and educational attainment (CR). The rs-fMRI analysis modeled the brain functional connectivity from the cholinergic basal forebrain (BF), the thalamus, and the visual network (VN), including bilateral calcarine, occipital superior, middle occipital, fusiform, inferior temporal, and middle temporal regions (Shirer et al., 2012). To test the specificity of the effects, we also considered the default mode network (DMN), including the posterior cingulum, precuneus, angular gyrus, thalamus, frontal medial orbitalis, frontal superior medial, temporal middle, and hippocampus (Shirer et al., 2012) and another control network (CNTR) including the parietal inferior, middle frontal, intraparietal, right caudate, frontal superior, frontal middle orbitalis, right supramarginal, left parietal superior, left temporal middle, left inferior temporal region.

The DPARSF toolbox was used to create individual seed-to-seed connectivity maps. Firstly, the mean regional time series was extracted from each seed region and correlated (Pearson's correlation) with that of the second seed region, which resulted in a square 5×5 correlation matrix. Then, Fisher's r-to-z transform was applied to standardize the resulting correlation values (Lowe et al., 1998). Fisher's z values were extracted for each pairwise functional connectivity for everyone. The spatial resolution of the present rsEEG spectral variables was relatively low (i.e., several centimeters), so the two hemispheres' homologous thalamus rs-fMRI connectivity values were averaged.

Specifically, the following rs-fMRI connectivity indexes were considered:

- Thalamus-BF as rs-fMRI connectivity values between thalamus and BF regions;
- VN as an average of the rs-fMRI connectivity values within all VN regions;
- Thalamus-VN as an average of the rs-fMRI connectivity values evaluated between the thalamus and each VN region (mean between left and right thalamus), and the average of the rs-fMRI connectivity values within all the VN regions;
- BF-VN: average of the rs-fMRI connectivity values evaluated between BF and each VN region, and the average of the rs-fMRI connectivity values within all the VN regions.

The same procedure was applied to DMN and CNTR networks.

2.6. Resting-state electroencephalographic (rsEEG) recordings

EEG data were recorded while the participants sat comfortably and relaxed with eyes closed in a standard resting state condition. At least 120 s of rsEEG (e.g., two periods of eyes-closed condition lasting 30 s each, intermingled with two periods of eyes-open condition) were acquired using a high-density 256-channel EGI system (Electrical Geodesics Inc., USA) with a sampling rate of 250 Hz and anti-aliasing bandpass analogic filtering. In this EGI system, the electrodes used are sponge-based to have a quick application time (10–20 min), which is ideal for seniors. Among the 256 electrodes, 224 electrodes cover the whole scalp. In contrast, the remaining ones are placed on the front, the top of the neck, and the face, allowing the measurement of electro-oculographic (EOG) and muscular electromyographic (EMG) activity. The impedances of all scalp electrodes were kept below 50 KΩ. The reference electrode was placed at the Cz site. A cephalic ground was used.

2.7. Spectral and quality analysis of the rsEEG data

In line with a previous study on the same rsEEG data (Babiloni et al., 2020a), we applied a semiautomatic "pruning" procedure of preliminary rsEEG data analysis to minimize the inter-individual variance of rsEEG rhythms to diminish 1) confounding effects of border electrodes with high impedance; 2) rsEEG data with residual artifacts provoked by the head or eye muscle activities; and 3) individual variability in the alpha frequency power peak (i.e., using individual alpha frequency peak, IAFp, as a benchmark; Klimesch, 1999; Gonzalez-Escamilla et al., 2015, 2016). With this procedure, blind to the amyloid status of the SMC seniors, two experts (Dr. Susanna Lopez and Prof. Claudio Del Percio) discarded individual rsEEG segments, single electrodes, or the whole rsEEG datasets with long periods (> 20 s) of irremediable artifacts. They considered in their analysis 68 scalp electrodes of the 10–10 montage system (i.e., AF7, AF3, AFz, AF4, AF8, FP1, FPz, FP2, F10, F9, F7, F5, F3, F1, Fz, F2, F4, F6, F8, FC5, FC3, FC1, FCz, FC2, FC4, FC6, FT9, FT7, FT8, Ft10, C5, C3, C1, C2, C4, C6, CP5, CP3, CP1, CPz, CP2, CP4, CP6, P9, T5-P7, P5, P3, P1, Pz, P2, P4, P6, T6-P8, P10, T9, TP7, T3-T7, T4-T8, TP8, T10, PO7, PO3, POz, PO4, PO8, O1, Oz and O2) from the whole array of 256 electrodes available.

After this "pruning" procedure, 105 SMCneg, and 56 SMCpos seniors with MMSE scores ≥ 28, accepted rsEEG datasets, and available rs-fMRI data were identified. rsEEG frequency bands of interest were individually determined based on the following frequency landmarks: the transition frequency (TF) and the IAFp (Klimesch et al., 1996, Klimesch, 1999, Klimesch et al., 1998). The TF marks the transition frequency between the theta and alpha bands, defined as the minimum rsEEG power density between 3 Hz and 8 Hz (i.e., between the delta and the alpha power peak). The IAFp is the maximum power density peak between 6 Hz and 14 Hz. The reference values to compute TF and IAFp on an individual basis were obtained by averaging rsEEG power density across Fz, Cz, Pz, O1, and O2 electrodes, which ensures the recording of scalp EEG signals with low biological noise (e.g., the scalp midline is relatively far from temporal and frontal muscles) and optimal electrical contacts using a standard EEG helmet. Furthermore, those selected electrodes were especially suitable for recording rsEEG rhythms at delta/theta (Fz and Cz) and alpha (Pz, O1, and O2) frequencies in our previous reference field studies (Babiloni et al., 2017, 2018, 2020b).

In detail, the following individual frequency bands were used in the present study considering a frequency resolution of 0.5 Hz:

- Delta from TF −4 Hz to TF −2 Hz.
- Theta from TF −2 Hz to TF.
- Alpha 1 from TF to the midpoint of the TF-IAFp range.
- Alpha 2 from the middle of the TF-IAFp range to IAFp.
- Alpha 3 from IAFp to IAFp + 2 Hz.

The above subdivision in alpha 1, alpha 2, and alpha 3 was performed for their different putative functions (for more clarifications, see Klimesch, 1999, and Pfurtscheller and Lopes da Silva, 1999). The rsEEG low-frequency alpha rhythms (alpha 1 and alpha 2) may denote the (de) synchronization of widespread cortical neural populations regulating the fluctuation of participants' global wakefulness and vigilance states (Klimesch, 1999). In contrast, the rsEEG high-frequency alpha rhythms (alpha 3) may denote the (de)synchronization of selective cortical neural populations processing modal-specific or semantic information during event-related paradigms (Klimesch, 1999; Pfurtscheller and Lopes da Silva, 1999).

In the present study, the mean TF was = 5.4 Hz (± 0.1 SE) in SMCneg and = 5.2 (± 0.1 SE) in SMCpos groups. The mean IAFp was = 9.3 Hz (± 0.2 SE) in the SMCneg group and = 9.2 Hz (± 0.1 SE) in the SMCpos group, with the maximum value of IAFp = 11 Hz. No statistically

significant differences between the two groups were observed for TF and IAFp (t-test, $p > 0.05$). Fixed beta 1 (13–20 Hz), beta 2 (20–30 Hz), and gamma (30–40 Hz) bands were also considered.

Five regions of interest (ROIs) were used considering the frontal, central, parietal, occipital, and temporal electrodes of the 10–10 electrode montage system. Specifically, these ROIs included the electrodes, as reported in Table Supplementary Material 1 (SM1; see Supplementary Materials). The evaluation of the whole-scalp topographic rsEEG patterns allowed us for an overall final quality evaluation and comparability of the results with previous studies.

2.8. Statistical analysis

The ANOVAs with Duncan test for post-hoc comparisons were performed by the commercial tool STATISTICA 10 (StatSoft Inc., www.statsoft.com). In contrast, the regression and moderation analyses with false discovery rate (FDR) for correcting for multiple comparisons were performed using R software (https://www.r-project.org/) to test the study hypotheses ($p < 0.05$). As the Kolmogorov-Smirnov test showed that several rsEEG power density distributions did not approximate to Gaussian distributions (null hypothesis of non-Gaussian distributions tested at $p < 0.05$), all rsEEG power density distributions underwent the log transformation and re-tested. The same procedure was used for the MRI data used as inputs for comparing SMC groups. The procedure's outcome approximated all rsEEG power density distributions to Gaussian distributions, allowing the use of the ANOVA models. The same was true for the MRI markers. As already transformed to Fisher's z values, rs-fMRI data did not undergo the normalization procedure. We checked for the achieved effect sizes and power of all the statistical analyses by the freeware G*Power 3.1.9.6 version (Faul et al., 2007, 2009).

2.9. Effect of brain amyloidosis and CR on posterior rsEEG alpha rhythms

The first statistical analysis was performed as a control analysis to evaluate the hypothesis that the posterior rsEEG power density at the individual alpha 2 and alpha 3 bands might differ between the Edu- and Edu+ sub-groups of the SMCneg and SMCpos seniors ($p < 0.05$), as shown in a previous reference study in the same cohort sub-sampling rsEEG activity based on 19 electrodes of the 10–20 electrode montage (Babiloni et al., 2020a).

To this aim, an ANOVA used the regional spectral rsEEG power density as a dependent variable. The ANOVA factors were Education (Edu- and Edu+), Group (SMCneg and SMCpos), Band (delta, theta, alpha 1, alpha 2, alpha 3, beta 1, beta 2, and gamma), and ROI (frontal, central, parietal, occipital, and temporal). The MRI markers resulting from being statistically different between the SMC sub-groups from the previous statistical analysis were used as covariates. The degrees of freedom were corrected by the Greenhouse-Geisser procedure when appropriate. For the planned contrasts, Duncan's test was used for post-hoc comparisons using a confirmatory statistical threshold of $p < 0.05$. The study hypothesis may be confirmed by a statistically significant ANOVA interaction among the factors Edu, Group, Band, and ROI ($p < 0.05$), associated with post-hoc solutions showing differences between the Edu- and Edu+ sub-groups for both SMCneg and SMCpos seniors in the alpha 2 and alpha 3 power density ($p < 0.05$, one tail). The significant effects of the above statistical analysis were controlled by the iterative (leave-one-out) Grubbs' test, detecting the presence of one or more outliers in the distribution of the regional rsEEG power density computed in the Edu- and Edu+ individuals for both SMCneg and SMCpos groups (Null hypothesis of non-Gaussian distributions tested at the arbitrary threshold of $p < 0.001$, to remove only individual values with high probability to be outliers and maintain the random sampling of the SMC population with the rsEEG features described above).

2.10. Effect of brain amyloidosis and CR on the association between the rs-fMRI connectivity in the extended resting-state brain networks and the posterior rsEEG alpha rhythms

The second statistical analysis was performed to evaluate the association between the mentioned rs-fMRI connectivity calculated in the extended resting-state brain networks and the posterior rsEEG alpha rhythms in the SMC participants. To this aim, several linear regression models were implemented (one model for each rsEEG and the corresponding rs-fMRI connectivity index) having the following features:

- Dependent rsEEG variables: parietal, occipital, temporal alpha 2 and alpha 3 spectral power density (one model for each variable);
- Predictors: Group (SMCneg, SMCpos), Education (Edu+, Edu-), rs-fMRI connectivity between the Thalamus/BF and the visual network, i.e., Thalamus-BF, Thalamus-VN, BF-VN), 2 and 3-way interactions among Group, Education, and rs-fMRI connectivity.

The corresponding models used the structural cortical thickness revealed by MRI measures in the parietal, occipital, and temporal regions as covariates. The study hypothesis may be confirmed by a statistically significant beta coefficient for each predictor and their 2 and 3-way interactions (i.e., the beta coefficient of the predictor is significantly different from zero, $p < 0.05$). The model accuracy was assessed by evaluating the residual standard error (RSE) and adjusted R-squared. The residuals' distribution was checked for heteroscedasticity, normality, and influential observations in the data ($p < 0.05$). The same statistical models were applied to the DMN and CNTR networks (see Supplementary Materials).

2.11. Moderation effect of brain amyloidosis and CR on the association between the rs-fMRI connectivity and the posterior rsEEG alpha rhythms

The third statistical analysis evaluated whether the brain amyloid deposition may moderate the association between the mentioned rs-fMRI connectivity and the posterior rsEEG alpha rhythms. This moderation effect may be, in turn, moderated by educational attainment as a proxy of CR. To this aim, we used the PROCESS tool available on https://haskayne.ucalgary.ca/CCRAM/resource-hub to perform the moderated moderation analysis. We limited the moderated moderation analyses only to statistically significant associations between the rs-fMRI connectivity of interest and the posterior rsEEG alpha power density, as evaluated by linear regression models, to make the results of the study as consistent as possible in the framework of the reported methodological limitations. This moderated moderation analysis included the following parameters for each of the following dependent variables:

- Dependent variable (one for each model): parietal, occipital, and temporal rsEEG alpha 3 power density;
- Independent variable: Visual Network (VN)-Thalamus rs-fMRI connectivity;
- Moderator variable 1: Group (SMCneg, SMCpos);
- Moderator variable 2: Educational attainment (Edu-, Edu+);
- Covariate: temporal thickness (only for the model involving the temporal rsEEG alpha 3 power density).

Specifically, we performed a moderated moderation analysis, which was equivalent to testing a 3-way interaction among the factors rs-fMRI connectivity, Group (SMCneg, SMCpos), and Education (Edu-, Edu+) considering both the Group and Education ($p < 0.05$) as moderators. The goodness of fit of all models on the rsEEG biomarkers was evaluated by Akaike Information Criterion (AIC). At the same time, the maximum likelihood estimation was obtained by the *nlminb* optimization method (Fox et al., 1978).

2.12. Effect of brain amyloidosis and CR on the association between the rs-fMRI connectivity in the VN and DMN and the posterior rsEEG alpha rhythms

The fourth statistical analysis used linear regression models ($p < 0.05$ uncorrected), testing the effect of the Group (SMCneg and SMCpos) and Education (Edu- and Edu+) predictors on the association between the rs-fMRI-based functional connectivity within the visual network (VN) and the rsEEG-dependent variables of interest, such as the parietal, occipital, and temporal rsEEG alpha 2 and alpha 3 power density.

2.13. Compensatory effect of CR on brain amyloidosis

The fifth statistical analysis tested the hypothesis of a CR compensatory effect on brain amyloid burden in SMCpos seniors. The regional and global PET SUVR values between the SMCneg and SMCpos groups were compared. The hypothesis was that the SMCpos seniors with higher CR (educational attainment) might be characterized by higher PET SUVR values, i.e., higher amyloid deposition, in several brain regions. To this aim, we performed an ANOVA having as dependent variable the regional PET SUVR values and as factors the Group (SMCneg, SMCpos), the Education (Edu-, Edu+), and the ROI (Left/Right Posterior Cingulum, Left/Right Inferior parietal lobe, Left/Right Precuneus, Left/Right Anterior Cingulum, Left/Right Superior frontal orbital lobe, and Left/Right Middle temporal lobe).

Fig. 1 illustrates the analytical plan followed in the present study, including SMC participant's enrolment, the amyPET, rs-fMRI, rsEEG, and core statistical procedures in the early preclinical stages of AD.

3. Results

3.1. Characterization of demographic, neuropsychological, and genetic markers in the SMCneg and SMCpos groups (based on amyloid PET biomarkers) and the effect of education attainment

Table 1 reports the relevant demographic, neuropsychological (MMSE score), and genetic (Apolipoprotein ε genotype, APOE) markers in the SMCneg Edu-, SMCneg Edu+, SMCpos Edu-, and SMCpos Edu+ sub-groups. It also reports the results of the statistical analyses ($p < 0.05$) computed to evaluate the presence or absence of statistically

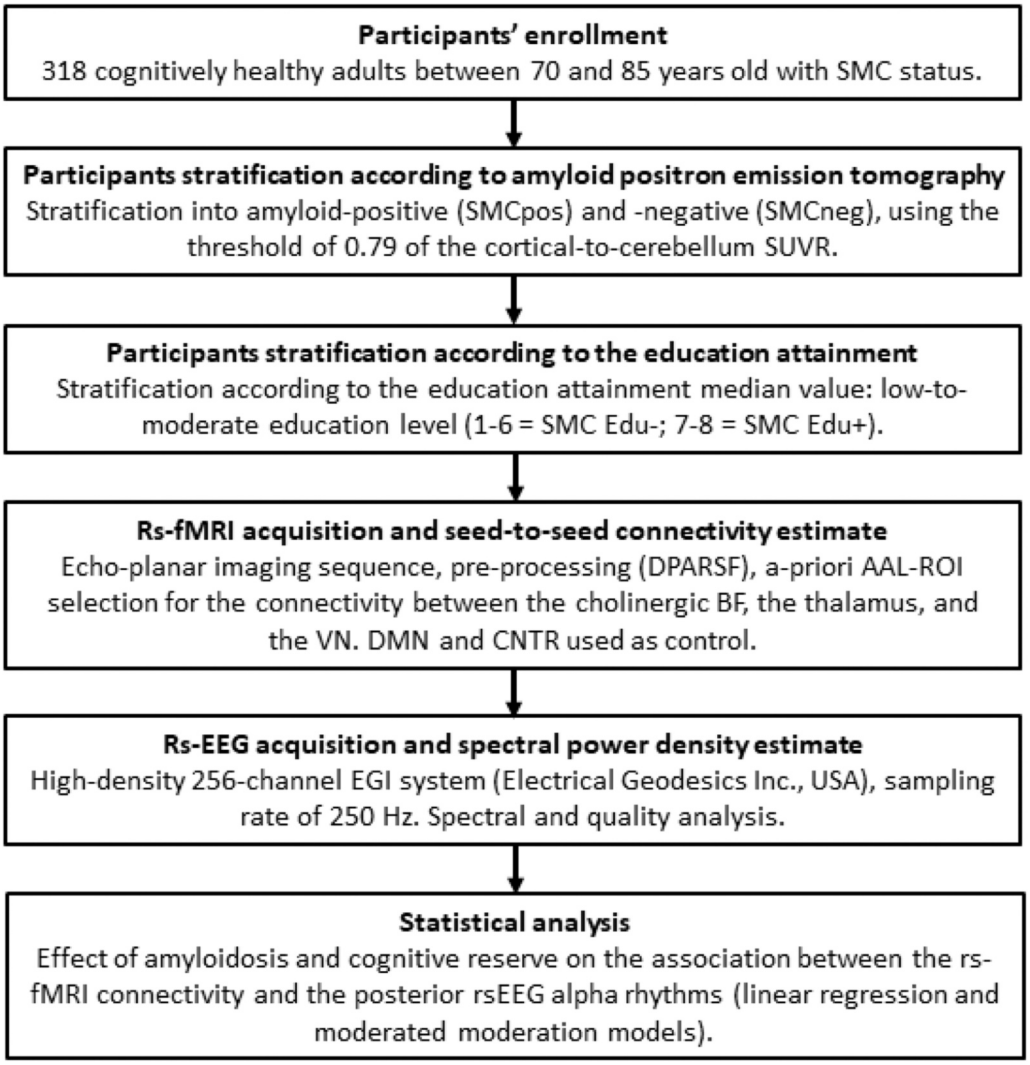

Fig. 1. *Flow-Chart Of The Analytical Plan Followed In The Present Study* It provides an overview of the amyPET, rs-fMRI, rsEEG, and core statistical procedures in the early preclinical stages of AD, characterizing the proposed advanced multimodal methodological approach based on participants' enrolment, molecular neuroimaging, functional neuroimaging, neurophysiology of brain rhythms, and statistical modeling. PET = Positron Emission Tomography; rs-fMRI = resting-state functional Magnetic Resonance Imaging; rsEEG = resting-state electroencephalography; SMC = subjective memory complaint; SUVR = standardized uptake value ratio; DPARSF = data processing assistant for resting-state fMRI; BF = basal forebrain; VN = **visual** network; DMN = default mode network; CNTR = control network.

Table 1
Demographic, Neuropsychological, And Genetic Data.

	SMCneg Edu-	SMCneg Edu+	SMCpos Edu-	SMCpos Edu+	Statistical analysis(Edu- VS Edu+)
N	49	56	30	26	-
Age	76.1 (±0.4 SE)	75.6 (±0.4 SE)	77.4 (±0.6 SE)	76.2 (±0.8 SE)	T-test: SMCneg: t-value (103) = 0.68, n.s. SMCpos: t-value (54) = 1.28, n.s.
Sex (M/F)	11/38	27/29	9/21	12/14	Fisher test: SMCneg: n.s.SMCpos: n.s.
Education	4.3 (±0.2 SE)	7.8 (±0.05 SE)	4.1 (±0.2 SE)	7.6 (±0.08 SE)	T-test: SMCneg: t-value (103) = −16.86,**p < 0.0001**SMCpos: t-value (54) = −14.48, **p < 0.0001**
MMSE	28.8 (±0.12 SE)	29.1 (±0.11 SE)	28.6 (±0.11 SE)	28.1 (±0.11 SE)	Mann Whitney U test: SMCneg: U = 1114.5, n. s.SMCpos: U = 330.0, n.s.
APOE genotype (N)	ε2/ε2 (1)ε2/ε3 (10), ε3/ε3 (33) ε2/ε4 (0)ε3/ε4 (5)ε4/ε4 (0)	ε2/ε2 (0)ε2/ε3 (6), ε3/ε3 (40)ε2/ε4 (1)ε3/ε4 (9)ε4/ε4 (0)	ε2/ε2 (0)ε2/ε3 (3), ε3/ε3 (16) ε2/ε4 (0)ε3/ε4 (9)ε4/ε4 (2)	ε2/ε2 (0)ε2/ε3 (2), ε3/ε3 (18)ε2/ε4 (0)ε3/ε4 (6)ε4/ε4 (0)	Chi-square test (2×5):SMCneg: Chi-square = 4.367, n.s.Chi-square test (2×4): SMCpos: Chi-square = 0.845, n.s.
APOE ε4 carriers/ non-carriers	5/44	10/56	11/19	6/26	Fisher test: SMCneg: n.s.SMCpos: n.s.

Table 1. Mean values (± standard error mean, SE) of the demographic, neuropsychological (MMSE score), and genetic (Apolipoprotein ε genotype, APOE) data, together with the results of their statistical comparisons ($p < 0.05$) in the groups of seniors with subjective memory complaint (SMC) found to be amyloid negative (SMCneg) and positive (SMCpos) to the marker of 'Alzheimer's amyloid neuropathology derived from 18 F-florbetapir positron emission tomography (amyPET). The SMC seniors were stratified according to lower (Edu-) or higher (Edu+) educational attainment. The SMC seniors with Edu+ received bachelor, 'master's degrees or Ph. D., while the SMC seniors with Edu- completed lower education programs. Legend: MMSE = Mini-Mental State Examination; M/F = males/females; APOE = Apolipoprotein E; n.s. = not significant ($p > 0.05$, uncorrected).

significant differences between the Edu- and Edu+ sub-groups for both SMCneg and SMCpos seniors as age (t-test), sex (Fisher test), education (t-test), MMSE score (Mann Whitney U test), APOE genotype (Chi-square test), and APOE ε4 carriers/non-carriers. Based on the stratification criterion, as expected, a statistically significant difference in education was found between the Edu- and Edu+ sub-groups for both SMCneg and SMCpos seniors considered separately ($p < 0.00001$). On the contrary, no statistically significant difference was found for the age, sex, MMSE score, APOE genotype, and APOE ε4 carriers/non-carriers between the Edu- and Edu+ sub-groups for both SMCneg and SMCpos seniors considered separately ($p > 0.05$).

3.2. Effect of the education attainment on the amyPET in the SMCneg and SMCpos groups

Fig. 2 illustrates the results of a statistically significant ANOVA 3-way interaction effect ($F(11, 1727) = 2.335$, $p = 0.008$) among the factors Group (SMCneg, SMCpos), Education (Edu-, Edu+), and ROI. The planned Duncan's post-hoc testing revealed higher values of the amyPET SUVR both at the regional and global levels in the SMCpos Edu+ group than in the SMCpos Edu- group ($p < 0.05$), in line with the assumption of compensatory processes associated with higher education attainment. In contrast, no difference was observed between the SMCneg Edu- and Edu+ groups. The analysis resulted in a partial-eta squared of 0.015, with an effect size of 0.12 and an achieved power of 0.95.

3.3. Effect of the education attainment on the structural MRI markers in the SMCneg and SMCpos groups

Table SM2 (see Supplementary Materials) reports the mean values (± SE) of the following eight relevant structural MRI markers for the Edu- and Edu+ sub-groups in the SMCneg and SMCpos seniors: 1) the normalized gray matter, white matter, and CSF volume (based on the total intracranial volume); 2) the adjusted hippocampal and BF volumes; and 3) the occipital, temporal, and inferior parietal cortical thicknesses. A statistically significant difference was found only in the SMCpos group for the temporal thickness ($p < 0.003$ uncorrected). It was lower in the Edu+ than the Edu- sub-groups, in line with compensatory processes associated with higher education attainment.

3.4. Effect of the education attainment on the posterior rsEEG alpha power density in the SMCneg and SMCpos groups

Figure 3 shows the mean values (± SE, log-transformed) of the regional rsEEG power density spectra for the Edu- and Edu+ sub-groups in the SMCneg and SMCpos seniors. The ANOVA showed a statistically significant 3-way interaction effect ($F(28, 4032) = 2.0204$, $p = 0.00116$; mean temporal thickness as a covariate) among the factors Group (SMCneg, SMCpos), Education (Edu-, Edu+), Band (delta, theta, alpha 1, alpha 2, beta 1, beta 2, and gamma), and ROI (frontal, central, parietal, occipital and temporal).

The Duncan planned post-hoc test ($p < 0.05$) showed that as compared to the SMCneg Edu- sub-group, the SMCneg Edu+ sub-group exhibited higher parietal ($p < 0.05$), occipital ($p < 0.0005$), and temporal ($p < 0.05$) rsEEG alpha 2 power density as well as higher occipital ($p < 0.01$) rsEEG alpha 3 power density, in line with a neuroprotective effect of CR.

The opposite effect was observed in the SMCpos group, in which Edu+ sub-groups showed lower frontal and occipital rsEEG alpha 2 ($p < 0.05$ and 0.005, respectively) and 3 ($p < 0.01$ and 0.05, respectively) power density as compared to the Edu- sub-group, in line with a compensatory effect of CR. The analysis resulted in a partial-eta squared of 0.014, with an effect size of 0.12 and an achieved power of 0.999.

Figure SM1 (see the Supplementary Materials) illustrates the topographic distribution of the alpha rsEEG power density at 8.5, 9.5, and 10.5 Hz as those frequency bins closer to the IAFp values in the SMCneg group (mean IAFp of 9.3 Hz, ± 0.2 SE) and in the SMCpos group (mean IAFp of 9.2 Hz ± 0.1 SE). The SMCneg Edu+ over the Edu- group showed a slightly higher rsEEG alpha power density, especially at 8.5 and 9.5 Hz frequency bins.

The above effects of the educational attainment were due to neither the presence of outliers (statistical threshold of Grubbs' test at $p < 0.001$; Figure SM2, see the Supplementary Materials) nor a different number of artifact-free rsEEG epochs included in the analysis (no statistically significant differences between the SMC Edu- and Edu+ groups according to t-test, $p > 0.05$).

3.5. Effect of covariates on the posterior rsEEG alpha power density in the SMCneg and SMCpos groups

Concerning the effect of the covariates on the rsEEG variables and their relationships with educational attainment, the results of the control regression analysis showed no statistically significant effect ($p >$

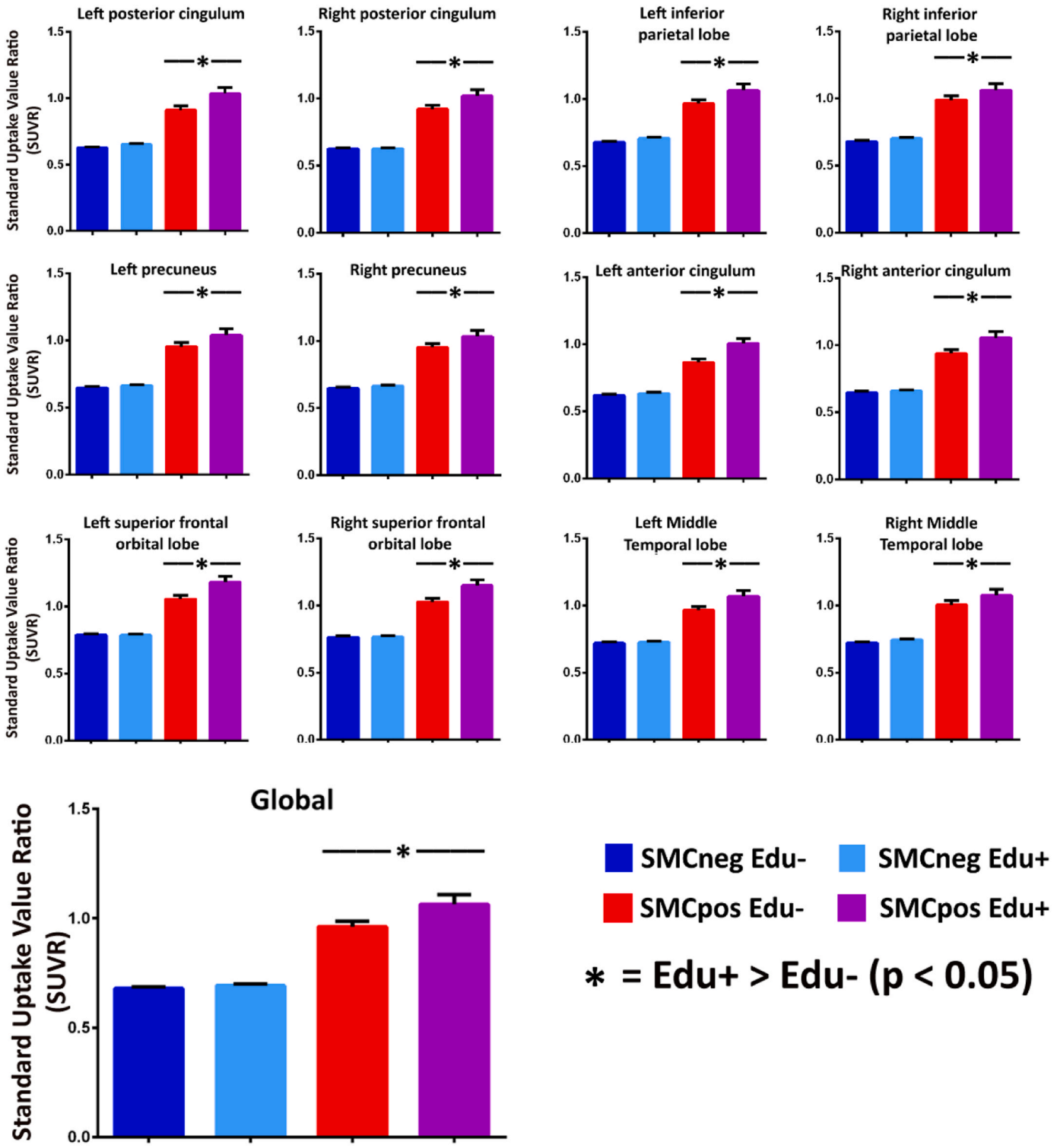

Fig. 2. *Regional Pattern Of AmyPET Standard Uptake Value Ratio (SUVR)*Mean values (± SE) of the regional patterns and global values of amyloid positron emission tomography (PET) standard uptake value ratio (SUVR), showing a statistically significant ANOVA interaction ($F(11, 1727) = 2.335$, $p = 0.008$) between the factors Group (SMCneg, SMCpos), Education (Edu-, Edu+) and ROI (Left/Right Posterior Cingulum, Left/Right Inferior parietal lobe, Left/Right Precuneus, Left/Right Anterior Cingulum, Left/Right Superior frontal orbital lobe, **and** Left/Right Middle temporal lobe). Duncan's post-hoc showed statistically higher SUVR values in subjective memory complaint (SMC) persons with Edu+ compared to SMC persons with Edu- ($p < 0.05$).

0.05) of the demographic, neuropsychological, genetic, and structural MRI variables on parietal and occipital rsEEG alpha 2 and alpha 3 power density. On the contrary, there was a statistically significant effect of the temporal thickness MRI variable on the temporal rsEEG alpha 2 and alpha 3 power density (Table SM3, see Supplementary Materials). Specifically, the intrahemispheric temporal thickness was lower in the SMCpos Edu+ group than in the Edu- group, in line with the compensatory processes associated with higher education attainment ($p < 0.05$). We reported the estimate of the β coefficients (± standard error of the mean, SE) in Table SM3, together with the p-values relative to the post-

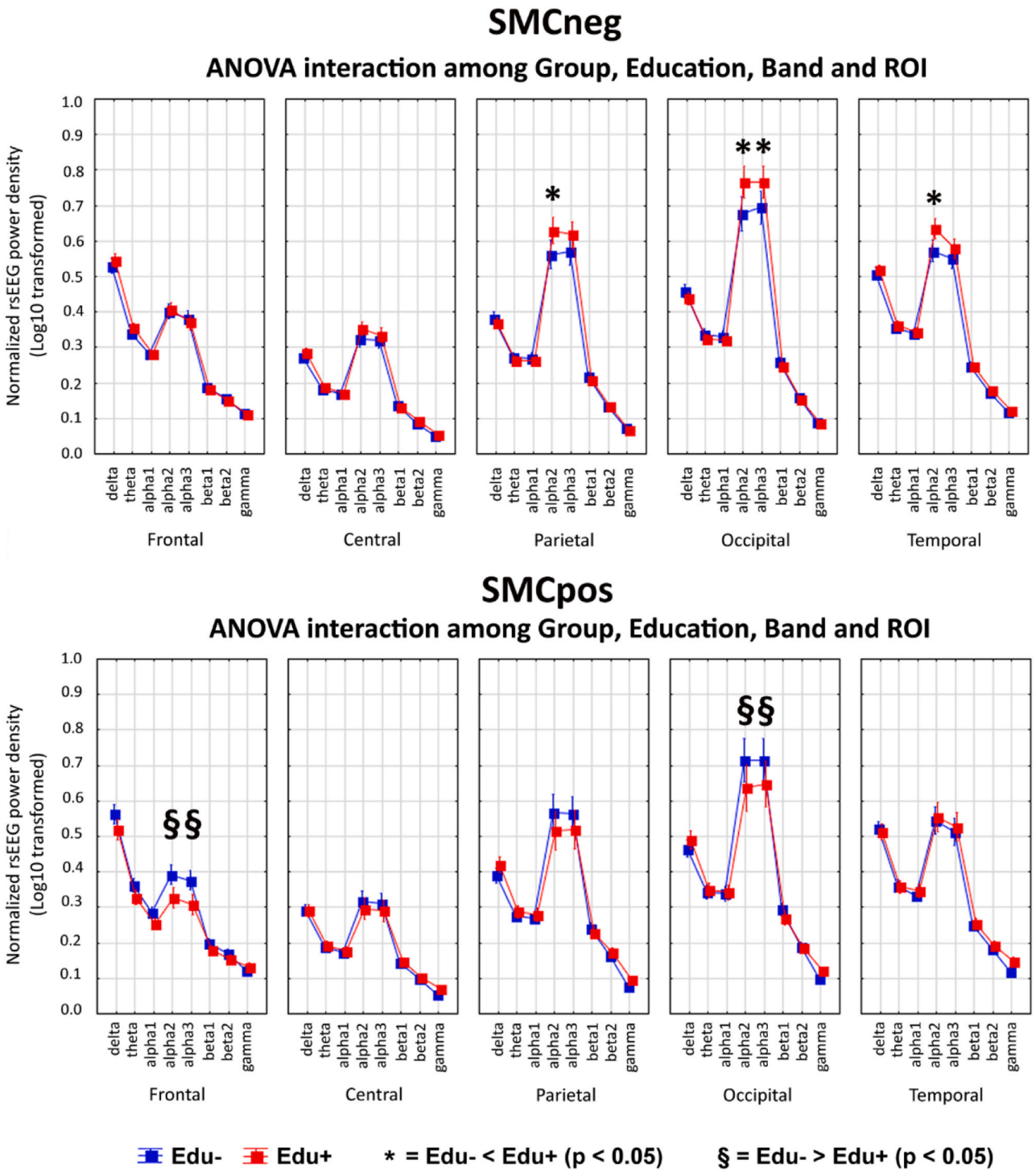

Fig. 3. *Effect Of Amyloidosis And Cognitive Reserve On Posterior Resting-State Electroencephalographic (rsEEG) Alpha Power Density.* Mean values (± standard error of the mean, SE, log-transformed) of normalized resting-state electroencephalographic (rsEEG) power density in persons with subjective memory complaint negative (SMCneg) and positive (SMCpos) to the biomarker for Alzheimer's disease amyloidosis in the brain measured by positron emission tomography (amyPET). More specifically, those values refer to 1) two groups (SMCneg and SMCpos seniors), 2) two education levels, namely lower and higher (Edu- and Edu+), 3) five regions of interest (ROIs; frontal, central, parietal, occipital, and temporal), and 4) eight frequency bands (delta, theta, alpha 1, alpha 2, alpha 3, beta 1, beta 2, and gamma). The ANOVA showed a statistically significant 3-way interaction effect ($F(28, 4032) = 2.0204$, $p = 0.00116$) among the factors Group, Education, Band, and ROI. The rectangles indicate the scalp regions and frequency bands in which the rsEEG power density presented a statistically significant pattern: Edu+ ≠ Edu- in the SMCneg and SMCpos senior groups (Duncan post hoc test, $p < 0.05$). The rsEEG results of the present study were based on the analysis performed from those 68 scalp electrodes of the 10–10 montage system.

hoc analysis (using FDR correction for multiple comparisons, $p < 0.05$).

3.6. Effect of the education attainment on rs-fMRI connectivity in the SMCneg and SMCpos groups

No statistically significant interaction effects were observed among Group, Education, and ROI factors ($p > 0.05$) for the rs-fMRI connectivity between the thalamus/BF and the resting-state cortical networks (VN, DMN, and CNTR). The Grubbs' test showed no outlier in the distribution of the rs-fMRI connectivity ($p < 0.001$; Figure 4). To describe available data analytically, we reported the rs-fMRI connectivity matrices in the four groups of participants among all the 119 regions in the Supplementary Materials (Figure SM3, see Supplementary Materials).

3.7. Effect of education attainment and brain amyloid accumulation on the association between rs-fMRI connectivity and posterior rsEEG alpha rhythms

As core findings of the present study, the linear regression models showed a statistically significant interacting effect of both Group (SMCneg and SMCpos) and Education (Edu- and Edu+) predictors on the positive association between the Thalamus-VN rs-fMRI connectivity and the posterior (parietal, temporal, and occipital) rsEEG alpha 3 power density ($p < 0.05$). Table 2 illustrates the details of these statistically significant results. These results are illustrated in Figure 5. For the SMCneg seniors, the Edu+ group showed a significantly positive association between the global vertical-horizontal Thalamus-VN rs-fMRI connectivity and the parietal, occipital, and temporal rsEEG alpha 3 power density ($p < 0.05$; FDR corrected). Along the same line, a statistically significant effect of the Group (SMCneg and SMCpos) predictor in the regression analysis unveiled the positive association between that "intrinsic" rs-fMRI connectivity within the VN nodes and the occipital rsEEG alpha 3 power density ($p < 0.05$; Table SM4, see the Supplementary Materials). Finally, the moderation analysis showed a statistically significant moderated moderation of Group and Education moderators on the above association between the VN-Thalamus rs-fMRI connectivity and the parietal, occipital, and temporal alpha 3 rsEEG power density ($p < 0.05$). In Table 3, the effect size of the moderated moderation effect, as estimated by R-squared change, evaluated by the test of highest-order unconditional interactions, is reported.

Notably, these effects could not be explained by the following biases. The Gaussian features, linearity, homoscedasticity, and lack of outliers in residuals' distributions were all confirmed ($p < 0.05$). The residual standard errors were low for all the above linear regression models, namely between 0.20 and 0.25. The mean temporal cortical thickness showed no statistically significant effect in the above models ($p > 0.05$).

Interesting secondary findings resulting from the control analysis of the study were the following. A statistically significant effect of the Group (SMCneg and SMCpos) predictor in the regression analysis unveiled the positive association between the BF-DMN rs-fMRI connectivity and the parietal and occipital rsEEG alpha 3 power density ($p < 0.05$; Table SM5, see the Supplementary Materials). For the SMCneg participants, there was a significant positive association between the BF-DMN rs-fMRI connectivity and the parietal rsEEG alpha 3 power density ($p < 0.05$; FDR corrected; Figure SM4, see the Supplementary Materials). In contrast, the opposite association was observed for the SMCpos participants, even if this effect was not statistically significant ($p > 0.05$). Furthermore, a statistically significant effect of the Group (SMCneg and SMCpos) predictor in the regression analysis unveiled the positive association between the "intrinsic" rs-fMRI connectivity within the DMN nodes and the occipital rsEEG alpha 3 power density ($p < 0.05$; Table SM4, see the Supplementary Materials).

No statistically significant effects were observed for the CNTR brain network ($p > 0.05$).

4. Discussion

In a previous study using the INSIGHT database collected in SMC persons (Dubois et al., 2018), CR (i.e., educational attainment) was associated with posterior rsEEG alpha rhythms (i.e., rsEEG power density) as a function of the brain amyloid deposition measured by ^{18}F-florbetapir PET (amyPET; Babiloni et al., 2020b). In the present exploratory study, the same database was re-investigated to test the

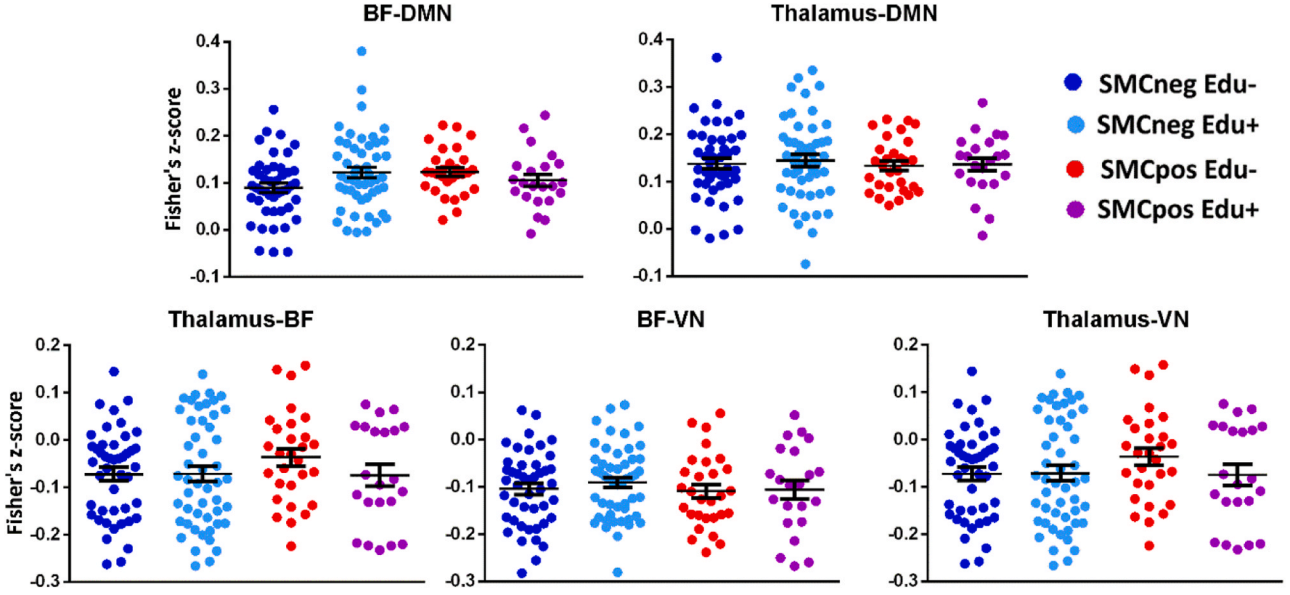

Fig. 4. *Resting-State Functional Magnetic Resonance Imaging (rs-fMRI) Connectivity In The Extended Resting-State Brain Networks.* Individual values of the global vertical-horizontal resting-state functional magnetic resonance imaging (rs-fMRI) connectivity involving the thalamus, BF, DMN, and VN. No statistically significant ANOVA interaction was observed among the factors Education (Edu- and Edu+), Group (SMCneg and SMCpos), and Node Pair (Thalamus-BF, Thalamus-DMN, Thalamus-VN for the first ANOVA; Thalamus-BF, BF-DMN, BF-VN for the second ANOVA; $p > 0.05$). Noteworthy, the Grubbs' test showed no outliers from those individual values of the intrahemispheric rs-fMRI connectivity (arbitrary threshold at $p < 0.001$). SMC = subjective memory complaint,VN = visual network, DMN = default mode network, BF = basal forebrain.

Table 2
Effect Of Amyloidosis And Cognitive Reserve On The Association Between The Resting-State Functional Magnetic Resonance Imaging (rs-fMRI) Connectivity And The Posterior Resting-State Electroencephalographic (RsEEG) Alpha Rhythms.

	F value	p-value	β coefficient	Standard Error
(a) Parietal alpha 3 rsEEG power density				
Intercept	0.9245	0.33814	0.52427	0.54524
Group	0.1127	0.73762	0.02632	0.07839
Education	2.6268	0.10759	0.11703	0.07221
Thalamus-VN	0.1771	0.67464	-0.20085	0.47733
Inferior Parietal Thickness	0.0074	0.93167	0.02024	0.23564
Group*Education	**3.8202**	**0.05**	**-0.24311**	**0.12438**
Group* Thalamus-VN	1.1103	0.29404	0.77204	0.73268
Education* Thalamus-VN	**4.1018**	**0.04**	**1.20467**	**0.59481**
Group*Education* Thalamus-VN	**5.4895**	**0.02**	**-2.45397**	**1.04737**
(b) Occipital alpha 3 rsEEG power density				
Intercept	0.0561	0.81312	0.16448	0.69427
Group	0.1926	0.66153	0.04125	0.09400
Education	3.1245	0.07956	0.15311	0.08662
Thalamus-VN	0.0679	0.79490	-0.14994	0.57555
Occipital Thickness	0.5831	0.44652	0.27176	0.35588
Group*Education	3.3739	0.06861	-0.27367	0.14899
Group* Thalamus-VN	1.1784	0.27978	0.94852	0.87379
Education* Thalamus-VN	3.2380	0.07436	1.28594	0.71463
Group*Education* Thalamus-VN	**5.1463**	**0.02501**	**-2.77174**	**1.22181**
(c) Temporal alpha 3 rsEEG power density				
Intercept	0.0074	0.93165	-0.04402	0.51223
Group	0.3757	0.54105	-0.03558	0.05804
Education	1.9689	0.16305	0.07497	0.05343
Thalamus-VN	0.0271	0.86951	-0.05840	0.35474
Temporal Thickness	1.3770	0.24285	0.22199	0.18918
Group*Education	0.4203	0.51800	-0.06123	0.09446
Group* Thalamus-VN	1.6126	0.20649	0.68561	0.53990
Education* Thalamus-VN	2.6183	0.10816	0.71263	0.44041
Group*Education* Thalamus-VN	**4.5614**	**0.03465**	**-1.61048**	**0.75406**

Table 2. Results of linear regression models showing the effect on the resting-state electroencephalographic (rsEEG) power density dependent variable (parietal, occipital, and temporal alpha 3rsEEG power density) of the following predictors: Group (SMCneg and SMCpos), Education (Edu- and Edu+), Parietal, Occipital, and Temporal Lobe Thickness, Thalamus-VN resting-state functional Magnetic Resonance Imaging (rs-fMRI) connectivity, and their 2- and 3-way interactions. Statistically significant effects are highlighted in red ($p < 0.05$; uncorrected). The rsEEG results of the present study were based on the analysis performed from those 68 scalp electrodes of the 10–10 montage system. VN = visual network.

novel hypothesis that posterior rsEEG alpha rhythms may be related to the rs-fMRI-based functional connectivity from (cholinergic) BF and thalamus to cortical visual networks supposed to be involved in the generation of those rhythms (Babiloni et al., 2020c). A particular interest was devoted to the possible interacting effects of the brain amyloid burden and CR (i.e., educational attainment). The multimodal methodological approach using molecular neuroimaging, structural and functional neuroimaging, and neurophysiological biomarkers allowed us to investigate the association between the posterior rsEEG alpha rhythms and the mentioned functional connectivity at an early stage of preclinical AD better to understand the brain reserve related to the CR in the disease model.

In the present study, the SMC participants showed more brain amyloidosis burden and temporal lobe atrophy when they had higher CR, in line with the assumption of the compensatory processes associated with high CR. These processes would avoid the manifestation of cognitive deficits despite brain neuropathology and neurodegeneration. Furthermore, the results showed a positive association between the rs-fMRI-based thalamic functional connectivity with the VN and the posterior rsEEG alpha rhythms in the SMC participants. Such an effect was affected by both brain amyloidosis and CR. In the SMC participants with high CR and negligible brain amyloidosis, the thalamic functional connectivity with the VN was positively correlated with the magnitude of the posterior rsEEG alpha rhythms. Notably, brain amyloidosis and CR moderated the association between the thalamic functional connectivity with the VN and those posterior rsEEG alpha rhythms.

The present results extend to a preclinical stage of AD previous rsEEG and magnetoencephalographic (MEG) evidence showing abnormal cortical functional connectivity, especially in the posterior cortical areas, in AD patients with prodromal (i.e., MCI) and overt clinical manifestations of dementia (Babiloni et al., 2008, 2009; Blinowska et al., 2017, Lopez et al., 2023; Koelewijn et al., 2017). Such abnormalities were further documented with higher spatial information content in rs-fMRI studies (Wang et al., 2021, Demirtaş et al., 2017; Skouras et al., 2019).

The present results also extend to a preclinical stage of AD previous multimodal rsEEG and rs-fMRI registrations showing that abnormalities in the rsEEG theta/alpha rhythms were associated with reduced rs-fMRI connectivity seeded in the posterior cortical areas in MCI patients with Alzheimer's pathological burden (Jovicich et al., 2019). Furthermore, there was a loss of the normal positive association between the rsEEG alpha rhythms and the rs-fMRI signal in the posterior cortex in patients with dementia due to AD neuropathology (Brueggen et al., 2017).

Keeping in mind these data, it can be speculated that the association between posterior rsEEG alpha rhythms and rs-fMRI-based functional connectivity in the thalamic and visual networks may represent a substantial aspect of the brain reserve associated with the CR (e.g., education attainment) in the SMC persons unaffected by the Alzheimer's amyloid pathology. Notably, they showed posterior rsEEG alpha rhythms higher compared to the SMC persons affected by Alzheimer's amyloid pathology and a certain medial temporal lobe atrophy. Therefore, such brain reserve might have a neuroprotective effect. As a novelty of the present results, this aspect of the brain reserve (i.e., the association between the rsEEG alpha rhythms and functional connectivity in the visual networks) may be affected by Alzheimer's amyloid pathology even at an early preclinical AD stage. However, at that stage, the brain reserve may still be able to compensate for Alzheimer's amyloid pathology. Indeed, the SMC persons affected by Alzheimer's amyloid pathology showed posterior rsEEG alpha rhythms lower compared to the SMC persons unaffected by that pathology. Along this speculative line, it can be hypothesized that brain reserve due to the CR may partially counteract the clinical effects of brain neurodegeneration and white-matter dysconnectivity in SMC persons, thus delaying the onset of MCI and dementia over time (Mortamais et al. 2014; Pettigrew et al., 2017). This hypothesis should be tested in future longitudinal studies using the present methodological approach.

The above data and speculations suggest that the brain reserve associated with high CR (e.g., education attainment) may be at least in part reflected by the association between the posterior rsEEG alpha rhythms and the functional connectivity within the visual network estimated from rs-fMRI signals. Along this line, previous multimodal rsEEG-rs-fMRI studies in healthy adults showed that these two neurophysiological correlates were related to each other. Parietal-occipital rsEEG alpha rhythms were associated with rs-fMRI signal in the thalamus and in cortical visual regions (Feige et al., 2005; Goldman et al., 2002; Gonçalves et al., 2006; Moosmann et al., 2003; Jaeger et al. 2023). Furthermore, the occipital rsEEG alpha reactivity during eye-opening was associated with the subcortical white-matter connectivity to the occipital cortex (Wan et al., 2019).

At the present early stage of the research, we cannot draw a conclusive interpretation of the neurophysiological mechanisms underlying the brain reserve due to high CR, reflected in an enhanced association between the posterior rsEEG alpha rhythms and the functional connectivity within the visual networks. We can only provide the following tentative neurophysiological model based on established neuroscientific knowledge. In the condition of resting state with eyes

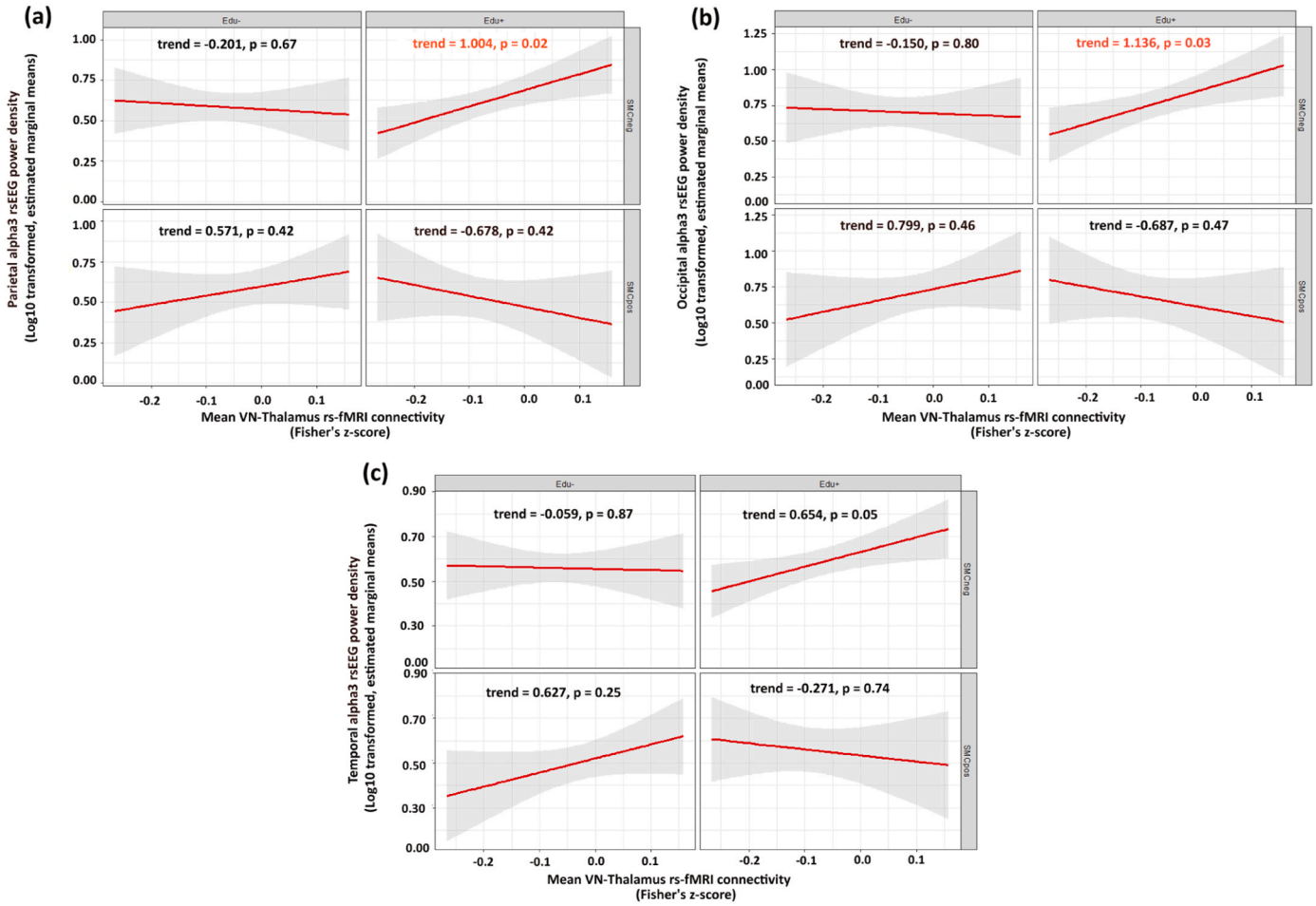

Fig. 5. *Effect Of Amyloidosis And Cognitive Reserve On The Association Between Thalamus-Visual Network (VN) rs-fMRI Connectivity And The Posterior rsEEG Alpha Rhythms In SMC Sub-Groups.* Plots of the parietal (upper left), occipital (upper right), and temporal (lower) resting-state electroencephalographic (rsEEG) alpha 3 power density (estimated marginal means by Linear Regression Model) in the subjective memory complaint (SMC)neg (left) and SMCpos (right) groups expressing the association with the Thalamus-VN resting-state functional magnetic resonance imaging (rs-fMRI) connectivity. Resting-state functional magnetic resonance imaging (rs-fMRI) connectivity values are defined as the bilateral 'Fisher's z-scores. Inside each graph, the statistically significant association calculated by the subgroup analysis using estimated marginal means are highlighted in red ($p < 0.05$; false discovery rate, FDR, corrected), as well as the slope coefficients and p-values. Illustrations are adjusted for inferior parietal and occipital thickness using estimated marginal means.

Table 3
Moderated Moderation Analysis.

Moderated Moderation model	Constant	Coefficient	t-value	p-value	LLCI	ULCI	R-squared change
(a) Parietal alpha 3 rsEEG power density							
VN-Thalamus XGroup X Edu	0.9245	0.33814	0.52427	0.54524	-4.2524	-0.4500	0.0398
(b) Occipital alpha 3 rsEEG power density							
VN-Thalamus XGroup X Edu	-2.7291	1.1641	-2.3443	0.0205	-5.0310	-0.4273	0. 0370
(c) Temporal alpha 3 rsEEG power density							
VN-Thalamus XGroup X Edu	-1.6105	0.7541	-2.1357	0.0347	-3.1029	-0.1181	0. 0330

Table 3. Results of the moderated moderation analysis on the association between the resting-state functional magnetic resonance imaging (rs-fMRI) connectivity and resting-state electroencephalographic (rsEEG) biomarkers using both Group (SMCneg, SMCpos) and Education (Edu-, Edu+) as moderators. Statistically significant associations are highlighted in red ($p < 0.05$). R-squared change values are reported to describe the test of highest-order unconditional interaction. Legend: LLCI: lower limit confidence interval at 95%; ULCI: upper limit confidence interval at 95%.

closed, dominant rsEEG alpha rhythms in posterior scalp regions would mainly reflect a global inhibition of the visual-spatial cortical regions through a significant 8–12 Hz oscillatory synchronization of the activity in diffuse neural populations within (visual-spatial) sensory thalamocortical as well as (visual-spatial) sensory and associative cortico-thalamic inhibitory and control circuits that (1) dampen the global arousal in posterior visual-spatial cortical areas and (2) gate and filter out irrelevant external sensory information during quiet levels of vigilance/consciousness with mind wandering, introspection, etc. and in task-related conditions (Klimesch, 1999; Pfurtscheller and Lopes da Silva, 1999; Pineda, 2005; Jansen and Mazaheri, 2010; Clayton et al., 2018; Babiloni et al., 2020c). Given the neurophysiological model of alpha rhythm generation, the present results suggest that in SMC persons with no significant brain amyloidosis, neuroprotective processes underpinning high CR may empower such synchronization in the 8–10 oscillatory activity of those brain neural populations generating the

dominant rsEEG alpha rhythms in posterior visual and visuospatial cortical areas, as inhibitory modulation of their cortical arousal from thalamocortical inputs. This empowered neurophysiological oscillatory mechanism might be neuroprotective for the brain and cognitive status along with aging (Jovicich et al., 2019; Babiloni et al., 2020a).

At the spatial macroscale level, it was previously shown that compared to SMC persons with low CR, those with high CR were characterized by a greater cerebral cortex thickness (Vaqué-Alcázar et al., 2017). Furthermore, the CR modulated the effects of subcortical lesions in the white matter on the risk of developing deficits from MCI to mild-to-moderate dementia in a large cohort of healthy older persons (Mortamais et al., 2014). Overall, CR may be associated with an ensemble of structural and functional neuroprotective factors that may delay the onset of cognitive deficits along with aging.

At the spatial mesoscale and microscale levels, neuroprotective processes underpinning the CR may induce a beneficial effect for AD on the neuronal membrane ionic channels and local thalamic circuits, generating rhythmic action potentials at the alpha frequency range. This circuit and the alpha rhythms would be modulated from cholinergic basal forebrain neurotransmission by after-depolarization potentials due to the opening of sodium ionic channels in those thalamocortical neurons (Hughes and Crunelli, 2005). Furthermore, the Pulvinar nucleus of the thalamus would modulate alpha rhythms in several posterior visual cortical areas concerning attention processes (Liu et al., 2012).

Considering the above neurophysiological model and the findings of the present study, we may speculate that in physiological conditions, neuroprotective processes underpinning the CR may promote plasticity, making more efficient the communication and coordination between glutamatergic corticothalamic pyramidal neurons, cholinergic basal forebrain neurons, and thalamocortical relay neurons, so preserving global cognitive status in aged persons (Nicolas et al., 2020). Its effect may be disrupted by Aβ neuropathology, which may impair metabotropic glutamatergic neurotransmission to cholinergic BF neurons with excitotoxicity due to abnormal calcium homeostasis (Gu et al., 2014).

4.1. Methodological limitations

The present results should be interpreted keeping in mind the methodological limitations discussed in the following paragraphs.

This is a monocentric clinical study with a relatively limited enrollment of SMC participants and relatively poor statistical power for their stratification based on brain amyloidosis and educational attainment. Indeed, the size effect of these findings may be relatively low due to the intrinsic variability of the posterior rsEEG alpha rhythms and the measures of rs-fMRI connectivity between the thalamus and visual cortical networks. This explanation would be supported by the relatively low-middle effect size achieved (it was measured by partial eta-squared for ANOVA and R-squared change for moderated moderation analysis). Therefore, we reported a statistical threshold with $p < 0.05$ corrected and an exploratory liberal threshold of $p < 0.05$ uncorrected for multiple comparisons. We did not preregister the study analytic plan in the public domain for its exploratory nature. For mature clinical studies, such registration is a good practice for transparency and replicability of experimental results.

The neuroimaging method for brain amyloid quantification was conservative to avoid false positive detection of AD neuropathology (i.e., it was chosen on its performance in distinguishing clinical AD from controls rather than for its detection of modestly but significantly elevated amyloid).

The study database included only rs-fMRI and rsEEG data recorded separately, so the association between the "true" associations between rs-fMRI functional connectivity and posterior rsEEG rhythms may be stronger and more extended from simultaneous rs-fMRI and rsEEG recordings.

Only baseline datasets were available in the enrolled SMC participants. Therefore, we could not experimentally test the "neuroprotective" and "compensatory" hypotheses following the evolution of the clinical status over time. In this article, we used those theoretical constructs for the tentative explanation of some effects observed in the rsEEG rhythms based on quoted literature findings.

Due to the limited human resources available, the EEG data were analyzed only at the scalp electrode level, and we could not perform a control whole-brain connectivity analysis from the rs-fMRI data.

Considering the above limitations, the present results should be cross-validated by a future multicentric, longitudinal study with (i) simultaneous rs-fMRI and rsEEG recordings performed in a larger cohort of SMC participants and (ii) more resources for data analysis and modeling. Such a study will allow (i) greater statistical power, (ii) a complementary whole-brain connectivity analysis from rsEEG-fMRI datasets, (iii) the analysis of rsEEG source activity and connectivity, and (iv) more conservative post-hoc tests with the correction for multiple comparisons.

In that future cross-validation study, the follow-ups will allow testing of the "neuroprotective" value of high posterior rsEEG alpha rhythms recorded in the SMCneg participants. The increased amplitude of these rhythms may predict a relatively stable SMC condition at long-term follow-ups. Similarly, the follow-ups will also allow testing of the "compensatory" processes inferred from low posterior rsEEG alpha rhythms recorded in the SMCpos participants with high CR (Edu+). The low amplitude of these rhythms, reflecting abnormal brain neural synchronization mechanisms compensated by the high CR, may predict a relatively fast decline from SMC to cognitive deficits at long-term follow-ups.

We are not in the position to perform whole-brain partial-last-square cross-validation in the EEG-fMRI datasets, so we are not able to modify the seed-to-seed connectivity approach. We hypothesize an association between posterior rsEEG rhythms and integrity of a "global" vertical-horizontal network involving the ascending cholinergic neuromodulatory systems, including BF and thalamus, and VN, which is in line with the seminal study by Wan et al. (2019).

The non-simultaneous acquisition of the rsEEG and fMRI signals and the intrinsic low spatial resolution of rsEEG techniques and global vertical-horizontal rs-fMRI connectivity approach limits this interpretation.

5. Conclusions

The present study tested the hypothesis that in SMC seniors, the association between the functional connectivity involving the (cholinergic) BF, thalamus, and visual cortical networks and the posterior rsEEG alpha rhythms may be affected by brain amyloid burden and educational attainment, as a proxy of CR.

The main results can be summarized as follows. In the SMC participants with lower brain amyloidosis and higher CR, there was a positive association between the thalamic functional connectivity with the VN and the posterior rsEEG alpha rhythms.

These results suggest that CR was associated with thalamocortical functional connectivity and arousal in the visual and visuospatial posterior cortical areas in cognitively unimpaired old persons, as revealed by rsEEG alpha rhythms. Alzheimer's disease neuropathology disrupted this CR influence. Overall, early AD stages with SMC may affect the thalamic-cortical neurophysiological oscillatory mechanisms underpinning the regulation of quiet vigilance/consciousness levels despite the CR. Notably, this dimension of the clinical manifestations is presently neglected and untreated in the AD clinical guidelines despite its well-known impact on patients' quality of life (Babiloni, 2022a). Future studies may use the present methodological multimodal approach to improve our brain's neurophysiological and connectome model of vigilance dysregulations in the early AD stages.

CRediT authorship contribution statement

Enrica Cavedo: Project administration, Investigation, Data curation. **Susanna Lopez:** Writing – review & editing, Writing – original draft, Validation, Methodology, Formal analysis, Data curation, Conceptualization. **Marie-Odile Habert:** Writing – review & editing, Project administration, Investigation, Data curation. **Gabriel González-Escamilla:** Writing – review & editing, Project administration, Investigation, Data curation. **Bruno Dubois:** Supervision, Project administration, Investigation, Funding acquisition, Data curation. **Hovagim Bakardjian:** Project administration, Investigation. **Fabrizio Stocchi:** Writing – review & editing, Validation. **Stefan J Teipel:** Writing – review & editing, Project administration, Investigation, Data curation. **Raffaele Ferri:** Writing – review & editing, Validation, Methodology. **Martin Dyrba:** Software, Formal analysis. **Giuseppe Noce:** Software, Formal analysis. **Michel J Grothe:** Project administration, Investigation, Data curation. **Marie-Claude Potier:** Project administration, Investigation. **Roberta Lizio:** Software, Formal analysis. **Patrizia Andrea Chiesa:** Writing – review & editing, Software, Formal analysis. **Pablo Lemercier:** Writing – review & editing, Software, Formal analysis. **Claudio Del Percio:** Writing – review & editing, Software, Formal analysis. **Giuseppe Spinelli:** Project administration, Investigation, Data curation. **Simone Lista:** Project administration, Investigation, Data curation. **Harald Hampel:** Writing – review & editing, Project administration, Investigation, Data curation. **Andrea Vergallo:** Project administration, Investigation, Data curation. **Claudio Babiloni:** Writing – review & editing, Supervision, Methodology, Conceptualization.

Acknowledgments

The research and this manuscript were part of the translational research program “PHOENIX,” awarded to Harald Hampel, administered by the Sorbonne University Foundation, and sponsored by la Fondation pour la Recherche sur Alzheimer.

The present study was developed based on the data of the INSIGHT-preAD project.

INSERM promoted the study in collaboration with ICM, IHU-A-ICM, and Pfizer and has received support within the "Investissement d′Avenir" (ANR-10-AIHU-06) French program. The study was promoted in collaboration with the "CHU de Bordeaux" (coordination CIC EC7), the promoter of the Memento cohort, funded by the Foundation Plan-Alzheimer. AVID/Lilly further supported the study.

CATI is a French neuroimaging platform funded by the French Plan Alzheimer (available at http://cati-neuroimaging.com).

The present study was developed based on the data of The PDWAVES Consortium (www.pdwaves.eu) and the PharmaCog project (https://www.imi.europa.eu/projects-results/project-factsheets/pharma-cog). The Partners and institutional affiliations are reported on the cover page of this manuscript.

In this study, the electroencephalographic (EEG) and clinical data analysis, the development of the statistical models, and the preparation of the iconography and the manuscript were partially supported by the following funds: (1) “Ricerca Corrente 2022–2023” attributed by the Italian Ministry of Health to the IRCCS Synlab SDN of Naples (Italy), Oasi Research Institute-IRCCS, Troina (Italy), and IRCCS San Raffaele Pisana of Rome (Italy); (2) the European Horizon project entitled "eBRAIN-Health (HORIZON-INFRA-2021-TECH-01, Grant Agreement: GAP-101058516); and (3) the Italian project entitled “Amyloid-related cortical excitability in patients with MCI due to Alzheimer’s disease” (PRIN-2022-PNRR, ID: 2022FJAXY8).

INSIGHT-preAD study group

Hovagim Bakardjian, Habib Benali, Hugo Bertin, Joel Bonheur, Laurie Boukadida, Nadia Boukerrou, Enrica Cavedo, Patrizia Chiesa, Olivier Colliot, Bruno Dubois, Marion Dubois, Stéphane Epelbaum, Geoffroy Gagliardi, Remy Genthon, Marie-Odile Habert, Harald Hampel, Marion Houot, Aurélie Kas, Foudil Lamari, Marcel Levy, Simone Lista, Christiane Metzinger, Fanny Mochel, Francis Nyasse, Catherine Poisson, Marie-Claude Potier, Marie Revillon, Antonio Santos, Katia Santos Andrade, Marine Sole, Mohmed Surtee, Michel Thiebaut de Schotten, Andrea Vergallo, Nadjia Younsi.

We thank Christiane Metzinger (ICM) for INSIGHT data management.

Dr. Susanna Lopez extracted the markers of electroencephalographic activity, while Dr. Patrizia Andrea Chiesa and Martin Dyrba extracted those of resting-state functional magnetic resonance imaging.

Disclosures

Dr. Harald Hampel is an employee of Eisai Inc. This work was performed during his previous position at Sorbonne University, Paris, France. At Sorbonne University, he was supported by the AXA Research Fund, the “*Fondation partenariale Sorbonne Université*” and the “*Fondation pour la Recherche sur Alzheimer*”, Paris, France. Dr. Harald Hampel serves as Senior Associate Editor for the Journal Alzheimer’s & Dementia, and has not received any fees or honoraria since May 2019; before May 2019, he had received lecture fees from Servier, Biogen, and Roche, research grants from Pfizer, Avid, and MSD Avenir (paid to the institution), travel funding from Eisai, Functional Neuromodulation, Axovant, Eli Lilly and Company, Takeda and Zinfandel, GE-Healthcare and Oryzon Genomics, consultancy fees from Qynapse, Jung Diagnostics, Cytox Ltd., Axovant, Anavex, Takeda and Zinfandel, GE Healthcare, Oryzon Genomics, and Functional Neuromodulation, and participated in scientific advisory boards of Functional Neuromodulation, Axovant, Eisai, Eli Lilly and Company, Cytox Ltd., GE Healthcare, Takeda and Zinfandel, Oryzon Genomics and Roche Diagnostics.

He is a co-inventor in several patents whose procedures were not used in the present study.

Dr. Enrica Cavedo is an employee of Qynapse SAS. This work was performed during her previous position at Sorbonne University, Paris, France.

Dr. Simone Lista received lecture honoraria from Roche and Servier.

AV declares no competing financial interests related to the present article, and his contribution to this article reflects only and exclusively his own academic expertise on the matter. This work was conceptualized and initiated during his previous academic position at Sorbonne University, Paris, France. AV was an employee of Eisai Inc. [Nov 2019 - June 2021]. AV does not receive any fees or honoraria since November 2019. Before November 2019 he had received lecture honoraria from Roche, MagQu LLC, and Servier.

Appendix A. Supporting information

Supplementary data associated with this article can be found in the online version at doi:10.1016/j.neurobiolaging.2024.02.008.

References

Arenaza-Urquijo, E.M., Wirth, M., Chételat, G., 2015. Cognitive reserve and lifestyle: moving towards preclinical Alzheimer’s disease. *Aug 10* Front Aging Neurosci. *7*, *134*. https://doi.org/10.3389/fnagi.2015.00134.

Babiloni, C., Barry, R.J., Başar, E., Blinowska, K.J., Cichocki, A., Drinkenburg, W.H.I.M., Klimesch, W., Knight, R.T., Lopes da Silva, F., Nunez, P., Oostenveld, R., Jeong, J., Pascual-Marqui, R., Valdes-Sosa, P., Hallett, M., 2020a. International Federation of Clinical Neurophysiology (IFCN) - EEG research workgroup: Recommendations on frequency and topographic analysis of resting state EEG rhythms. Part 1: Applications in clinical research studies (Jan). Clin. Neurophysiol. *131* (*1*), *285–307*. https://doi.org/10.1016/j.clinph.2019.06.234.

Babiloni C., Blinowska K., Bonanni L., Cichocki A., De Haan W., Del Percio C., Dubois B., Escudero J., Fernández A., Frisoni G., Guntekin B., Hajos M., Hampel H., Ifeachor E., Kilborn K., Kumar S., Johnsen K., Johannsson M., Jeong J., LeBeau F., Lizio R., Lopes da Silva F., Maestú F., McGeown W.J., McKeith I., Moretti D.V., Nobili F., Olichney J., Onofrj M., Palop J.J., Rowan M., Stocchi F., Struzik Z.M., Tanila H., Teipel S., Taylor J.P., Weiergräber M., Yener G., Young-Pearse T., Drinkenburg W.H., Randall F. What electrophysiology tells us about Alzheimer’s disease: a window into the

synchronization and connectivity of brain neurons. Neurobiol Aging. 2020c *Jan;85*: *58-73*. doi: 10.1016/j.neurobiolaging.2019.09.008.

Babiloni, C., Del Percio, C., Lizio, R., Noce, G., Cordone, S., Lopez, S., Soricelli, A., Ferri, R., Pascarelli, M.T., Nobili, F., Arnaldi, D., Aarsland, D., Orzi, F., Buttinelli, C., Giubilei, F., Onofrj, M., Stocchi, F., Stirpe, P., Fuhr, P., Gschwandtner, U., Ransmayr, G., Caravias, G., Garn, H., Sorpresi, F., Pievani, M., Frisoni, G.B., D'Antonio, F., De Lena, C., Güntekin, B., Hanoğlu, L., Başar, E., Yener, G., Emek-Savaş, D.D., Triggiani, A.I., Franciotti, R., De Pandis, M.F., Bonanni, L., 2017. Abnormalities of cortical neural synchronization mechanisms in patients with dementia due to Alzheimer's and Lewy body diseases: an EEG study. Neurobiol. Aging *55*, *143–158*. https://doi.org/10.1016/j.neurobiolaging.2017.03.030.

Babiloni, C., Del Percio, C., Lizio, R., Noce, G., Lopez, S., Soricelli, A., Ferri, R., Nobili, F., Arnaldi, D., Famà, F., Aarsland, D., Orzi, F., Buttinelli, C., Giubilei, F., Onofrj, M., Stocchi, F., Stirpe, P., Fuhr, P., Gschwandtner, U., Ransmayr, G., Garn, H., Fraioli, L., Pievani, M., Frisoni, G.B., D'Antonio, F., De Lena, C., Güntekin, B., Hanoğlu, L., Başar, E., Yener, G., Emek-Savaş, D.D., Triggiani, A.I., Franciotti, R., Taylor, J.P., Vacca, L., De Pandis, M.F., Bonanni, L., 2018b. Abnormalities of resting-state functional cortical connectivity in patients with dementia due to Alzheimer's and Lewy body diseases: an EEG study. Neurobiol. Aging *65*, *18–40* (May).

Babiloni, C., Del Percio, C., Lizio, R., Noce, G., Lopez, S., Soricelli, A., Ferri, R., Pascarelli, M.T., Catania, V., Nobili, F., Arnaldi, D., Famà, F., Aarsland, D., Orzi, F., Buttinelli, C., Giubilei, F., Onofrj, M., Stocchi, F., Vacca, L., Stirpe, P., Fuhr, P., Gschwandtner, U., Ransmayr, G., Garn, H., Fraioli, L., Pievani, M., Frisoni, G.B., D'Antonio, F., De Lena, C., Güntekin, B., Hanoğlu, L., Başar, E., Yener, G., Emek-Savaş, D.D., Triggiani, A.I., Franciotti, R., Taylor, J.P., De Pandis, M.F., Bonanni, L., 2018a. Abnormalities of resting state cortical eeg rhythms in subjects with mild cognitive impairment due to Alzheimer's and Lewy Body Diseases. J. Alzheimers Dis. *62* (*1*), *247–268*. https://doi.org/10.3233/JAD-170703.

Babiloni, C., Ferri, R., Noce, G., Lizio, R., Lopez, S., Lorenzo, I., Panzavolta, A., Soricelli, A., Nobili, F., Arnaldi, D., Famà, F., Orzi, F., Buttinelli, C., Giubilei, F., Cipollini, V., Marizzoni, M., Güntekin, B., Aktürk, T., Hanoğlu, L., Yener, G., Özbek, Y., Stocchi, F., Vacca, L., Frisoni, G.B., Del Percio, C., 2021. Abnormalities of Cortical Sources of Resting State Alpha Electroencephalographic Rhythms are Related to Education Attainment in Cognitively Unimpaired Seniors and Patients with Alzheimer's Disease and Amnesic Mild Cognitive Impairment. Cereb. Cortex *31* (*4*), *2220–2237*. *Mar 5*.

Babiloni, C., Lopez, S., Del Percio, C., Noce, G., Pascarelli, M.T., Lizio, R., Teipel, S.J., González-Escamilla, G., Bakardjian, H., George, N., Cavedo, E., Lista, S., Chiesa, P.A., Vergallo, A., Lemercier, P., Spinelli, G., Grothe, M.J., Potier, M.C., Stocchi, F., Ferri, R., Habert, M.O., Fraga, F.J., Dubois, B., Hampel, H., 2020b. INSIGHT-preAD *S*tudy Group. Resting-state posterior alpha rhythms are abnormal in subjective memory complaint seniors with preclinical Alzheimer's neuropathology and high education level: the INSIGHT-preAD study. *Feb 1* Neurobiol. Aging *pii: S0197-4580* (*20*), *30026–30029*. https://doi.org/10.1016/j.neurobiolaging.2020.01.012.

Babiloni, C., Lorenzo, I., Lizio, R., Lopez, S., Tucci, F., Ferri, R., Soricelli, A., Nobili, F., Arnaldi, D., Famà, F., Buttinelli, C., Giubilei, F., Cipollini, V., Onofrj, M., Stocchi, F., Vacca, L., Fuhr, P., Gschwandtner, U., Ransmayr, G., Aarsland, D., Parnetti, L., Marizzoni, M., D'Antonio, F., De Lena, C., Güntekin, B., Yıldırım, E., Hanoğlu, L., Yener, G., Gündüz, D.H., Taylor, J.P., Schumacher, J., McKeith, I., Frisoni, G.B., De Pandis, M.F., Bonanni, L., Percio, C.D., Noce, G., 2022b. Reactivity of posterior cortical electroencephalographic alpha rhythms during eyes opening in cognitively intact older adults and patients with dementia due to Alzheimer's and Lewy body diseases. Neurobiol. Aging *115*, *88–108* (Jul).

Babiloni, C., 2022a. The dark side of Alzheimer's Disease: neglected physiological biomarkers of brain hyperexcitability and abnormal consciousness level. J. Alzheimers Dis. *88* (*3*), *801–807*. https://doi.org/10.3233/JAD-220582.

Bennett, D.A., Arnold, S.E., Valenzuela, M.J., Brayne, C., Schneider, J.A., 2014. Cognitive and social lifestyle: links with neuropathology and cognition in late life (Jan). Acta Neuropathol. *127* (*1*), *137–150*. https://doi.org/10.1007/s00401-013-1226-2.

Bozzali, M., Dowling, C., Serra, L., Spanò, B., Torso, M., Marra, C., Castelli, D., Dowell, N. G., Koch, G., Caltagirone, C., Cercignani, M., 2015. The impact of cognitive reserve on brain functional connectivity in Alzheimer's disease. J. Alzheimers Dis. *44* (*1*), *243–250*. https://doi.org/10.3233/JAD-141824.

Brueggen, K., Fiala, C., Berger, C., Ochmann, S., Babiloni, C., Teipel, S.J., 2017. Early Changes in alpha band power and dmn bold activity in Alzheimer's disease: a simultaneous resting state EEG-fMRI study. *Oct 6* Front Aging Neurosci. *9*, *319*. https://doi.org/10.3389/fnagi.2017.00319.

Buchman, A.S., Bennett, D.A., 2012. Amyloid pathology in persons with "normal" cognition. *Jan 24* Neurology *78* (*4*), *228–229*. https://doi.org/10.1212/WNL.0b013e31824367c2.

Cammisuli, D.M., Franzoni, F., Scarfò, G., Fusi, J., Gesi, M., Bonuccelli, U., Daniele, S., Martini, C., Castelnuovo, G., 2022. What Does the Brain Have to Keep Working at Its Best? Resilience Mechanisms Such as Antioxidants and Brain/Cognitive Reserve for Counteracting Alzheimer's Disease Degeneration. *Apr 24* Biology *11* (*5*), *650*. https://doi.org/10.3390/biology11050650.

Cavedo, E., Chiesa, P.A., Houot, M., Ferretti, M.T., Grothe, M.J., Teipel, S.J., Lista, S., Habert, M.O., Potier, M.C., Dubois, B., Hampel, H., 2018. INSIGHT-preAD Study Group; Alzheimer Precision Medicine Initiative (APMI). Sex differences in functional and molecular neuroimaging biomarkers of Alzheimer's disease in cognitively normal older adults with subjective memory complaints. Alzheimers Dement *14* (*9*), 1204–1215. https://doi.org/10.1016/j.jalz.2018.05.014.

Cecchetti G., Agosta F., Basaia S., Cividini C., Cursi M., Santangelo R., Caso F., Minicucci F., Magnani G., Filippi M. *Resting-state electroencephalographic biomarkers of Alzheimer's disease. Neuroimage Clin.* 2021;*31:102711*. doi: 10.1016/j.nicl.2021.102711.

Chiesa, P.A., Cavedo, E., Grothe, M.J., Houot, M., Teipel, S.J., Potier, M.C., Habert, M.O., Lista, S., Dubois, B., Hampel, H., 2019a. INSIGHT-preAD Study Group and the Alzheimer Precision Medicine Initiative (APMI). Relationship between Basal Forebrain Resting-State Functional Connectivity and Brain Amyloid-β Deposition in Cognitively Intact Older Adults with Subjective Memory Complaints (Jan). Radiology *290* (*1*), *167–176*. https://doi.org/10.1148/radiol.2018180268.

Chiesa, P.A., Cavedo, E., Vergallo, A., Lista, S., Potier, M.C., Habert, M.O., Dubois, B., Thiebaut de Schotten, M., Hampel, H., 2019b. INSIGHT-preAD study group; Alzheimer Precision Medicine Initiative (APMI). Differential default mode network trajectories in asymptomatic individuals at risk for Alzheimer's disease (Jul). Alzheimers Dement *15* (*7*), *940–950*. https://doi.org/10.1016/j.jalz.2019.03.006.

Clark, C.M., Pontecorvo, M.J., Beach, T.G., Bedell, B.J., Coleman, R.E., Doraiswamy, P. M., Fleisher, A.S., Reiman, E.M., Sabbagh, M.N., Sadowsky, C.H., Schneider, J.A., Arora, A., Carpenter, A.P., Flitter, M.L., Joshi, A.D., Krautkramer, M.J., Lu, M., Mintun, M.A., Skovronsky, D.M., 2012. AV-45-A16 Study Group. Cerebral PET with florbetapir compared with neuropathology at autopsy for detection of neuritic amyloid-β plaques: a prospective cohort study. In: . *Lancet Neurol. 2012 Aug;11*(*8*): *669-78. Epub 2012 Jun 28. Erratum in: Lancet Neurol*, *11*, p. *658*. https://doi.org/10.1016/S1474-4422(12)70142-4.

Clayton, M.S., Yeung, N., Cohen Kadosh, R., 2018. The many characters of visual alpha oscillations (Oct). Eur. J. Neurosci. *48* (*7*), *2498–2508*. https://doi.org/10.1111/ejn.13747.

Dubois, B., Epelbaum, S., Nyasse, F., Bakardjian, H., Gagliardi, G., Uspenskaya, O., Houot, M., Lista, S., Cacciamani, F., Potier, M.C., Bertrand, A., Lamari, F., Benali, H., Mangin, J.F., Colliot, O., Genthon, R., Habert, M.O., Hampel, H., 2018. INSIGHT-preAD study group. Cognitive and neuroimaging features and brain β-amyloidosis in individuals at risk of Alzheimer's disease (INSIGHT-preAD): a longitudinal observational study. Lancet Neurol. *17* (*4*), *335–346*. https://doi.org/10.1016/j.clinph.2019.06.007.

Feige, B., Scheffler, K., Esposito, F., Di Salle, F., Hennig, J., Seifritz, E., 2005. Cortical and subcortical correlates of electroencephalographic alpha rhythm modulation (May). J. Neurophysiol. *93* (*5*), *2864–2872*. https://doi.org/10.1152/jn.00721.2004.

Fleck, J.I., Arnold, M., Dykstra, B., Casario, K., Douglas, E., Morris, O., 2019. Distinct Functional Connectivity Patterns Are Associated With Social and Cognitive Lifestyle Factors: Pathways to Cognitive Reserve. *Nov 13* Front Aging Neurosci. *11*, *310*. https://doi.org/10.3389/fnagi.2019.00310.

Fleck, J.I., Kuti, J., Mercurio, J., Mullen, S., Austin, K., Pereira, O., 2017. The impact of age and cognitive reserve on resting-state brain connectivity. *Dec 1* Front Aging Neurosci. *9*, *392*. https://doi.org/10.3389/fnagi.2017.00392.

Foubert-Samier, A., Catheline, G., Amieva, H., Dilharreguy, B., Helmer, C., Allard, M., Dartigues, J.F., 2012. Education, occupation, leisure activities, and brain reserve: a population-based study. Neurobiol Aging (Feb), *33* (*2*), *423*. https://doi.org/10.1016/j.neurobiolaging.2010.09.023 (Feb).

Franzmeier, N., Duering, M., Weiner, M., Dichgans, M., Ewers, M., 2017b. Alzheimer's Disease Neuroimaging Initiative (ADNI). Left frontal cortex connectivity underlies cognitive reserve in prodromal Alzheimer disease. Neurology *88* (*11*), *1054–1061*. https://doi.org/10.1212/WNL.0000000000003711.

Franzmeier, N., Düzel, E., Jessen, F., Buerger, K., Levin, J., Duering, M., Dichgans, M., Haass, C., Suárez-Calvet, M., Fagan, A.M., Paumier, K., Benzinger, T., Masters, C.L., Morris, J.C., Perneczky, R., Janowitz, D., Catak, C., Wolfsgruber, S., Wagner, M., Teipel, S., Kilimann, I., Ramirez, A., Rossor, M., Jucker, M., Chhatwal, J., Spottke, A., Boecker, H., Brosseron, F., Falkai, P., Fliessbach, K., Heneka, M.T., Laske, C., Nestor, P., Peters, O., Fuentes, M., Menne, F., Priller, J., Spruth, E.J., Franke, C., Schneider, A., Kofler, B., Westerteicher, C., Speck, O., Wiltfang, J., Bartels, C., Araque Caballero, M.Á., Metzger, C., Bittner, D., Weiner, M., Lee, J.H., Salloway, S., Danek, A., Goate, A., Schofield, P.R., Bateman, R.J., Ewers, M., 2018b. Left *f*rontal hub connectivity delays cognitive impairment in autosomal-dominant and sporadic Alzheimer's disease. Brain *141* (*4*), *1186–1200*. https://doi.org/10.1093/brain/awy008.

Franzmeier, N., Göttler, J., Grimmer, T., Drzezga, A., Áraque-Caballero, M.A., Simon-Vermot, L., Taylor, A.N.W., Bürger, K., Catak, C., Janowitz, D., Müller, C., Duering, M., Sorg, C., Ewers, M., 2017a. Resting-state connectivity of the left frontal cortex to the default mode and dorsal attention network supports reserve in mild cognitive impairment. Front Aging Neurosci. *9*, *264*. https://doi.org/10.3389/fnagi.2017.00264.

Franzmeier, N., Hartmann, J., Taylor, A.N.W., Araque-Caballero, M.Á., Simon-Vermot, L., Kambeitz-Ilankovic, L., Bürger, K., Catak, C., Janowitz, D., Müller, C., Ertl-Wagner, B., Stahl, R., Dichgans, M., Duering, M., Ewers, M., 2018a. The left frontal cortex supports reserve in aging by enhancing functional network efficiency. Alzheimers Res Ther. *10* (*1*), *28*. https://doi.org/10.1186/s13195-018-0358-y.

Friston, K.J., Williams, S., Howard, R., Frackowiak, R.S., Turner, R., 1996. Movement-related *effects in fMRI time-series* (Mar). Magn. Reson Med. *35* (*3*), *346–355*. https://doi.org/10.1002/mrm.1910350312.

Garibotto, V., Borroni, B., Kalbe, E., Herholz, K., Salmon, E., Holtoff, V., Sorbi, S., Cappa, S.F., Padovani, A., Fazio, F., Perani, D., 2008. Education and occupation as proxies for reserve in aMCI converters and AD: FDG-PET evidence. *Oct 21* Neurology *71* (*17*), *1342–1349*. https://doi.org/10.1212/01.wnl.0000327670.62378.c0.

Goldman, R.I., Stern, J.M., Engel Jr, J., Cohen, M.S., 2002. Simultaneous EEG *and* fMRI *of the alpha rhythm.*. *Dec 20* Neuroreport *13* (*18*), *2487–2492*. https://doi.org/10.1097/01.wnr.0000047685.08940.d0.

Gonçalves, S.I., de Munck, J.C., Pouwels, P.J., Schoonhoven, R., Kuijer, J.P., Maurits, N. M., Hoogduin, J.M., Van Someren, E.J., Heethaar, R.M., Lopes da Silva, F.H., 2006. Correlating *the alpha rhythm to BOLD using simultaneous EEG/fMRI: inter-subject variability* (Mar). Neuroimage *30* (*1*), *203–213*. https://doi.org/10.1016/j.neuroimage.2005.09.062.

Gonzalez-Escamilla, G., Atienza, M., Cantero, J.L., 2015. Impaired cortical oscillatory coupling in mild cognitive impairment: anatomical substrate and ApoE4 effects. Brain Struct. Funct. *220* (*3*), *1721–1737*. https://doi.org/10.1007/s00429-014-0757-1.

Gonzalez-Escamilla, G., Atienza, M., Garcia-Solis, D., Cantero, J.L., 2016. Cerebral and blood correlates of reduced functional connectivity in mild cognitive impairment (Jan). Brain Struct. Funct. *221* (*1*), *631–645*. https://doi.org/10.1007/s00429-014-0930-6.

Gu, Z., Cheng, J., Zhong, P., Qin, L., Liu, W., Yan, Z., 2014 Oct 8. Aβ selectively impairs mGluR7 modulation of NMDA signaling in basal forebrain cholinergic neurons: implication in Alzheimer's disease. J. Neurosci. *34* (*41*), *13614–13628*. https://doi.org/10.1523/JNEUROSCI.1204-14.2014.

Habert, M.O., Bertin, H., Labit, M., Diallo, M., Marie, S., Martineau, K., Kas, A., Causse-Lemercier, V., Bakardjian, H., Epelbaum, S., Chételat, G., Houot, M., Hampel, H., Dubois, B., Mangin, J.F., 2018. INSIGHT-AD study group. Evaluation of amyloid status in a cohort of elderly individuals with memory complaints: Validation of the method of quantification and determination of positivity thresholds. Ann. Nucl. Med *32* (*2*), *75–86*. https://doi.org/10.1007/s12149-017-1221-0.

Hampel, H., Lista, S., Neri, C., Vergallo, A., 2019. Time for the systems-level integration of aging: Resilience enhancing strategies to prevent Alzheimer's disease (Oct). Prog. Neurobiol. *181*, 101662. https://doi.org/10.1016/j.pneurobio.2019.101662.

Hughes, S.W., Crunelli, V., 2005. Thalamic mechanisms of EEG alpha rhythms and their pathological implications (Aug). Neuroscientist *11* (*4*), *357–372*. https://doi.org/10.1177/1073858405277450.

Jaeger, C., Nuttall, R., Zimmermann, J., Dowsett, J., Preibisch, C., Sorg, C., Wohlschlaeger, A., 2023. Targeted rhythmic visual stimulation at individual participants' intrinsic alpha frequency causes selective increase of occipitoparietal BOLD-fMRI and EEG functional connectivity. *Apr 15* Neuroimage *270*, 119981. https://doi.org/10.1016/j.neuroimage.2023.119981.

Jovicich, J., Babiloni, C., Ferrari, C., Marizzoni, M., Moretti, D.V., Del Percio, C., Lizio, R., Lopez, S., Galluzzi, S., Albani, D., Cavaliere, L., Minati, L., Didic, M., Fiedler, U., Forloni, G., Hensch, T., Molinuevo, J.L., Bartrés Faz, D., Nobili, F., Orlandi, D., Parnetti, L., Farotti, L., Costa, C., Payoux, P., Rossini, P.M., Marra, C., Schönknecht, P., Soricelli, A., Noce, G., Salvatore, M., Tsolaki, M., Visser, P.J., Richardson, J.C., Wiltfang, J., Bordet, R., Blin, O., 2019. Frisoniand GB; and the pharmacog consortium.two-year longitudinal monitoring of amnestic mild cognitive impairment patients with prodromal alzheimer's disease using topographical biomarkers derived from functional magnetic resonance imaging and electroencephalographic activity. J. Alzheimers Dis. *69* (*1*), *15–35*. https://doi.org/10.3233/JAD-180158.

Klimesch, W., Doppelmayr, M., Russegger, H., Pachinger, T., 1996. Theta band power in the human scalp eeg and the encoding of new information. *May 17* Neuroreport *7* (*7*), *1235–1240*. https://doi.org/10.1097/00001756-199605170-00002.

Klimesch, W., Russegger, H., Doppelmayr, M., Pachinger, T., 1998. A method for the calculation of induced band power: implications for the significance of brain oscillations (Mar). Electro Clin. Neurophysiol. *108* (*2*), *123–130*. https://doi.org/10.1016/s0168-5597(97)00078-6.

Klimesch, W., 1999. EEG alpha and theta oscillations reflect cognitive and memory performance: a review and analysis. Brain Res. Rev. *29*, *169–195*. https://doi.org/10.1016/s0165-0173(98)00056-3.

Kouzuki, M., Asaina, F., Taniguchi, M., Musha, T., Urakami, K., 2013. The relationship between the diagnosis method of neuronal dysfunction (DIMENSION) and brain pathology in the early stages of Alzheimer's disease (Jun). Psychogeriatrics *13* (*2*), *63–70*. https://doi.org/10.1111/j.1479-8301.2012.00431.x.

Liu, Y., Julkunen, V., Paajanen, T., Westman, E., Wahlund, L.O., Aitken, A., Sobow, T., Mecocci, P., Tsolaki, M., Vellas, B., Muehlboeck, S., Spenger, C., Lovestone, S., Simmons, A., Soininen, H., 2012. AddNeuroMed Consortium. Education increases reserve against Alzheimer's disease–evidence from structural MRI analysis. Neuroradiology *54* (*9*), *929–938*. https://doi.org/10.1007/s00234-012-1005-0.

Lowe, M.J., Mock, B.J., Sorenson, J.A., 1998. Functional connectivity in single and multislice echoplanar imaging using resting-state fluctuations (Feb). Neuroimage *7* (*2*), *119–132*. https://doi.org/10.1006/nimg.1997.0315.

Moosmann, M., Ritter, P., Krastel, I., Brink, A., Thees, S., Blankenburg, F., Taskin, B., Obrig, H., Villringer, A., 2003. Correlates of alpha rhythm in functional magnetic resonance imaging and near infrared spectroscopy (Sep). Neuroimage *20* (*1*), *145–158*. https://doi.org/10.1016/s1053-8119(03)00344-6.

Morbelli, S., Nobili, F., 2014. Cognitive reserve and clinical expression of Alzheimer's disease: evidence and implications for brain PET imaging. Am. J. Nucl. Med Mol. Imaging *4* (*3*), *239–247. Apr 25*.

Mortamais, M., Portet, F., Brickman, A.M., Provenzano, F.A., Muraskin, J., Akbaraly, T. N., Berr, C., Touchon, J., Bonafé, A., le Bars, E., Menjot de Champfleur, N., Maller, J. J., Meslin, C., Sabatier, R., Ritchie, K., Artero, S., 2014. Education modulates the impact of white matter lesions on the risk of mild cognitive impairment and dementia (Nov). Am. J. Geriatr. Psychiatry *22* (*11*), *1336–1345*. https://doi.org/10.1016/j.jagp.2013.06.002.

Nicolas, B., Alessandra, D., Daniela, P., Osman, R., Sara, T., Giovanni, B.F., Valentina, G., 2020. Alzheimer's Disease Neuroimaging Initiative. Basal forebrain metabolism in Alzheimer's disease continuum: relationship with education (Mar). Neurobiol. Aging *87*, *70–77*. https://doi.org/10.1016/j.neurobiolaging.2019.11.013.

Pettigrew, C., Soldan, A., 2019. Defining cognitive reserve and implications for cognitive aging. *Jan 9* Curr. Neurol. Neurosci. Rep. *19* (*1*), *1*. https://doi.org/10.1007/s11910-019-0917-z.

Pfurtscheller, G., Lopes da Silva, F.H., 1999. Event-related EEG/MEG synchronization and desynchronization: basic principles (Nov). Clin. Clin. Neurophysiol. *110* (*11*), *1842–1857*. https://doi.org/10.1016/s1388-2457(99)00141-8.

Pineda, J.A., 2005. The functional significance of mu rhythms: translating "seeing" and "hearing" into "doing.". *Dec 1* Brain Res Brain Res Rev. *50* (*1*), *57–68*. https://doi.org/10.1016/j.brainresrev.2005.04.005.

Reed, B.R., Mungas, D., Farias, S.T., Harvey, D., Beckett, L., Widaman, K., Hinton, L., DeCarli, C., 2010. Measuring cognitive reserve based on the decomposition of episodic memory variance (Aug). Brain *133* (*Pt 8*), *2196–2209*. https://doi.org/10.1093/brain/awq154.

Sachdev, P.S., Valenzuela, M., 2009. Brain and cognitive reserve (Mar). Am. J. Geriatr. Psychiatry *17* (*3*), *175–178*. https://doi.org/10.1097/JGP.0b013e318196a661.

Serra, L., Musicco, M., Cercignani, M., Torso, M., Spanò, B., Mastropasqua, C., Giulietti, G., Marra, C., Bruno, G., Koch, G., Caltagirone, C., Bozzali, M., 2015. Cognitive reserve and the risk for Alzheimer's disease: a longitudinal study (Feb). Neurobiol. Aging *36* (*2*), *592–600*. https://doi.org/10.1016/j.neurobiolaging.2014.10.010.

Shirer, W.R., Ryali, S., Rykhlevskaia, E., Menon, V., Greicius, M.D., 2012. Decoding *subject-driven cognitive states with whole-brain connectivity patterns* (Jan). Cereb. Cortex *22* (*1*), *158–165*. https://doi.org/10.1093/cercor/bhr099.

Smailovic, U., Koenig, T., Kåreholt, I., Andersson, T., Kramberger, M.G., Winblad, B., Jelic, V., 2018. Quantitative EEG power and synchronization correlate with Alzheimer's disease CSF biomarkers (Mar). Neurobiol. Aging *63*, *88–95*. https://doi.org/10.1016/j.neurobiolaging.2017.11.005.

SternY.Arenaza-UrquijoE.M., Bartrés-FazD.BellevilleS, CantilonM.Chetelat, G.Ewers, M. Franzmeier, N.Kempermann, G.Kremen, W.S.Okonkwo, O.Scarmeas, N.Soldan, A. Udeh-Momoh, C.Valenzuela, M.Vemuri, P.Vuoksimaa, E.2018 , Reserve, Resilience and Protective Factors PIA empirical definitions and conceptual frameworks workgroupWhite.: Defin. Invest. Cogn. Reserve, brain Reserve, brain Maint. Alzheimers Dementpii: S1552-526018334913349510.1016/j.jalz.2018.07.219.

Teipel, S.J., Cavedo, E., Lista, S., Habert, M.O., Potier, M.C., Grothe, M.J., Epelbaum, S., Sambati, L., Gagliardi, G., Toschi, N., Greicius, M.D., Dubois, B., Hampel, Hs, 2018. INSIGHT-preAD study group; Alzheimer Precision Medicine Initiative (APMI). Effect of Alzheimer's disease risk and protective factors on cognitive trajectories in subjective memory complainers: an INSIGHT-preAD study (Sep). Alzheimers Dement *14* (*9*), *1126–1136*. https://doi.org/10.1016/j.jalz.2018.04.004.

Thomas, B.A., Erlandsson, K., Modat, M., Thurfjell, L., Vandenberghe, R., Ourselin, S., Hutton, B.F., 2011. The importance of appropriate partial volume correction for PET quantification in Alzheimer's disease. Eur. J. Nucl. Med Mol. Imaging *38* (*6*), *1104–1119*. https://doi.org/10.1007/s00259-011-1745-9.

Tzourio-Mazoyer, N., Landeau, B., Papathanassiou, D., Crivello, F., Etard, O., Delcroix, N., Mazoyer, B., Joliot, M., 2002. Automated anatomical labeling of activations in SPM using a macroscopic anatomical parcellation of the MNI MRI single-subject brain (Jan). Neuroimage *15* (*1*), *273–289*. https://doi.org/10.1006/nimg.2001.0978.

Valenzuela, M.J., Sachdev, P., 2006. Brain reserve and cognitive decline: a non-parametric systematic review (Aug). Psychol. Med *36* (*8*), *1065–1073*. https://doi.org/10.1017/S0033291706007744.

Vaqué-Alcázar, L., Sala-Llonch, R., Valls-Pedret, C., Vidal-Piñeiro, D., Fernández-Cabello, S., Bargalló, N., Ros, E., Bartrés-Faz, D., 2017. Differential age-related gray and white matter impact mediates educational influence on elders' cognition. Brain Imaging Behav. *11* (*2*), *318–332*. https://doi.org/10.1007/s11682-016-9584-8.

Wan, L., Huang, H., Schwab, N., Tanner, J., Rajan, A., Lam, N.B., Zaborszky, L., Li, C.R., Price, C.C., Ding, M., 2019. From eyes-closed to eyes-open: Role of cholinergic projections in EC-to-EO alpha reactivity revealed by combining EEG and MRI. *Feb 1* Hum. Brain Mapp. *40* (*2*), *566–577*. https://doi.org/10.1002/hbm.24395.

Yan, C.G., Wang, X.D., Zuo, X.N., Zang, Y.F., 2016. DPABI: data processing & analysis for (resting-state) brain imaging. Neuroinformatics *14*, *339–351*. https://doi.org/10.1007/s12021-016-9299-4.

Zahodne, L.B., Manly, J.J., Brickman, A.M., Narkhede, A., Griffith, E.Y., Guzman, V.A., Schupf, N., Stern, Y., 2015. Is residual memory variance a valid method for quantifying cognitive reserve? A longitudinal application (Oct). Neuropsychologia *77*, *260–266*. https://doi.org/10.1016/j.neuropsychologia.2015.09.009.

Zahodne, L.B., Manly, J.J., Brickman, A.M., Siedlecki, K.L., Decarli, C., Stern, Y., 2013. Quantifying cognitive reserve in older adults by decomposing episodic memory variance: replication and extension (Sep). J. Int Neuropsychol. Soc. *19* (*8*), *854–862*. https://doi.org/10.1017/S1355617713000738.